Environmental Science
Water Research & Technology

Removal and Growth of Microorganisms across Treatment and Simulated Distribution at a Pilot-Scale Direct Potable Reuse Facility

Journal:	*Environmental Science: Water Research & Technology*
Manuscript ID	EW-ART-12-2019-001087.R1
Article Type:	Paper

Title: Removal and Growth of Microorganisms across Treatment and Simulated Distribution at a Pilot-Scale Direct Potable Reuse Facility

Authors: Scott E. Miller[1,2], Roberto A. Rodriguez[3], and Kara L. Nelson[1,2,*]

[1]Department of Civil and Environmental Engineering, College of Engineering, University of California, Berkeley, CA, United States;

[2]National Science Foundation Engineering Research Center for Re-inventing the Nation's Urban Water Infrastructure, Berkeley, CA, United States;

[3]School of Public Health, University of Texas Health Sciences Center at Houston, TX, United States

Corresponding author email: karanelson@berkeley.edu

Abstract

Multi-barrier advanced treatment trains have been shown to purify wastewater to drinking water standards, but improved methods are needed to better understand microbial concentrations, viability, and growth potential throughout treatment and distribution systems. In this study, bulk water cell counts, adenosine triphosphate concentrations, and assimilable organic carbon were measured throughout a pilot-scale direct potable reuse facility and three parallel chlorinated simulated distribution systems fed with the pilot's finished water. We also investigated the impacts of treatment operations (e.g., membrane cleanings) and perturbations (e.g., incomplete wastewater nitrification) on microbial water quality. Intact cell counts and total adenosine triphosphate

concentrations were reduced to near or below method quantification limits (22 cells/mL and 10^{-4} nM, respectively) by reverse osmosis and advanced oxidation. Total cell counts and assimilable organic carbon concentrations were consistently above method quantification limits (12 cells/mL and 10 μg/L, respectively) in finished water (i.e., granular activated carbon filtrate). However, assimilable organic carbon levels in finished water were lower than values typically measured in conventional drinking water systems in the United States, and cell counts were dramatically reduced by batch chlorination. Occasional ammonia passage through advanced treatment caused large variations in chlorine demand in finished water, and a strong inverse correlation was observed between cell counts and residual free chlorine in the simulated distribution systems. We show that multi-barrier advanced treatment reliably rejects wastewater-derived bacterial cells, and that the methods applied herein can provide complementary information to traditional monitoring approaches to evaluate microbial water quality throughout treatment and distribution.

Water Impact Statement: Purification of wastewater can provide water-stressed regions a reliable drinking water supply. We evaluated and provided recommendations for the use of enhanced analytical tools to assess microbial water quality in an advanced treatment train and simulated distribution systems, with the aim to further improve the microbial safety of potable reuse.

Key words: advanced water treatment, log removal values, flow cytometry, ATP, assimilable organic carbon, chlorine residual

1. Introduction

Increasing pressures from population growth, urbanization, and climate change are challenging many cities' water security. For arid cities in the southwestern United States (e.g., El Paso, Texas), aggravated droughts in recent years have intermittently reduced freshwater reservoir levels to less than 10% of maximum capacity [1]. There is growing recognition that direct potable reuse, i.e., the deliberate introduction of purified wastewater into a drinking water treatment facility or distribution system, can produce high-quality water to diversify municipal water portfolios, reduce imports, and meet future demand. Direct potable reuse requires extensive advanced treatment of wastewater, which most often involves combinations of ozonation, granular activated carbon filtration (GAC), microfiltration (MF), reverse osmosis (RO) or nanofiltration (NF), and a H2O2-UV advanced oxidation process (AOP) [2].

Finished water from advanced treatment trains has been shown to meet water quality regulations for potable reuse [3-5], but knowledge gaps remain regarding how individual treatment processes alter microbial water quality. In particular, it is unclear how final treatment steps (e.g., chemical conditioning or GAC filtration) influence microbial abundance and regrowth of finished and distributed waters. Furthermore, advanced treatment facilities almost always monitor total organic carbon, but rarely measure assimilable organic carbon (AOC), which is the fraction of labile dissolved carbon that can be most rapidly utilized by heterotrophic microorganisms [6]. AOC has been linked to microbial growth in drinking water [7] and non-potable reuse systems [8], but the role of residual AOC in potable reuse systems has not been specifically assessed. Measurement of AOC and the numbers and viability of microorganisms across different potable reuse treatment trains could provide insight into the performance and ideal sequencing of treatment processes to manage microbial numbers and growth potential.

Recent sequencing-based studies of potable reuse treatment trains by Stamps et al. (2018) and Kantor et al. (2019) reported that advanced treatment substantially reduces the proportion of the treated water microbial taxa that is shared with wastewater, but there have been no studies to date investigating microbial abundance and viability in continuous-flow drinking water distribution systems fed with advanced treated wastewater [9,10]. The results herein complement the findings of Kantor et al. (2019), which are from the same pilot system. Previous studies of distribution systems fed with conventionally-sourced waters treated by NF or RO report substantial microbial growth despite oligotrophic conditions in the treated water [11-13]. A recent lab-scale study that simulated non-continuous, build-scale plumbing in the context of direct potable reuse reported that conventional drinking water and potable reuse scenarios yielded equivalent microbial regrowth, but the proportion of organisms that were viable was not quantified [14]. There remains a need to evaluate microbial growth and viability in distribution systems under continuous-flow conditions and under more potable reuse blend ratios. There is also a research gap regarding the effectiveness of different chlorine residual types (i.e., free vs. combined chlorine) and concentrations at suppressing microbial numbers and activity in potable reuse distribution systems. In general, lower growth and microbial numbers in distributed water may be expected in potable reuse scenarios due to lower concentrations of AOC and suspended solids.

Several emerging methods for evaluating microbial water quality, including fluorescence-based flow cytometric assays for enumerating total and intact microbial cells, a luminescence-based assay for measuring adenosine tri-phosphate (ATP), and a flow cytometry-based bioassay for quantifying AOC, have successfully been used for evaluating microbial growth and viability in conventional drinking water treatment and distribution systems [15-19]. Previous studies have shown cell counts determined by flow cytometry to be more reproducible and informative, and to

correlate more strongly with ATP, than traditional microbial quantification methods such as heterotrophic plate counts [17,20-22]. Moreover, as cultivation-independent methods, flow cytometry and intracellular ATP quantify nearly all organisms present in a sample and are more applicable to the low-biomass effluents of treatment processes like MF, RO, AOP, and chlorination. Lastly, the flow cytometry-based bioassay for measuring AOC [23] has been applied by researchers to drinking water treatment trains [24-27], but to our knowledge has not yet been applied across an entire advanced treatment facility.

In this study we aimed to determine the effects of advanced water treatment processes on microbial numbers, viability, and growth potential in the context of direct potable reuse. Specifically, we quantified bulk water cell counts, ATP, and AOC across a pilot-scale advanced treatment facility and three bench-scale simulated drinking water distribution systems. The impact of operations (e.g., membrane cleanings) and treatment perturbations (e.g., incomplete nitrification at the wastewater facility) on microbial water quality were also investigated. Finally, we consider the utility and feasibility of deploying the assays used herein to full-scale advanced treatment facilities. This work is unique in applying enhanced analytical methods to understand advanced treatment processes that will be integral components of many future potable reuse treatment trains. We also discuss implications for the management of microbial water quality during distribution, which has been a crucial and understudied aspect of potable reuse systems.

2. Study Site, Methods, and Materials

2.1 Layout of the pilot-scale direct potable reuse facility and bulk water sampling

We studied a pilot-scale advanced treatment facility in El Paso, Texas that was operated from June 8, 2015 to January 29, 2016 with a treatment capacity of 5.3 x 10^5 L/day. To determine optimal

full-scale treatment train design, several treatment steps were evaluated with parallel treatment processes that were fed equal flows. The advanced treatment train is illustrated in **Figure 1**, and major treatment processes are described in detail in the **Supplementary Methods**. Briefly, raw wastewater was treated by a conventional activated sludge facility designed to fully nitrify influent ammonia; however, the facility often failed to fully nitrify ammonia during high loading periods. Unchlorinated secondary wastewater effluent was then treated sequentially by ozonation (target concentration of 3.5 mg/L), chloramination to limit membrane biofouling (target concentration 2 – 4 mg/L as Cl_2), parallel microfiltration and ultrafiltration (MF and UF; 0.1 and 0.04 μm nominal pore sizes, respectively), parallel reverse osmosis (RO) or nanofiltration (NF), a H_2O_2-UV advanced oxidation process (AOP; UV dose of 840 mJ/cm^2 and H_2O_2 dose of 4 mg/L), and granular activated carbon filtration (GAC). We also collected, transported, and chlorinated GAC filtrate that was then fed to three bench-scale, parallel storage reservoirs ("Reservoir") and parallel simulated distribution systems (SDS), as discussed further below. We collected grab bulk water samples from the pilot facility's secondary wastewater feed, after every major treatment process (including after each individual process that were in parallel; e.g., both MF and UF filtrates), and from the bench-scale reservoirs and SDS from October 2015 through January 2016. Data for parallel processes are often aggregated and presented herein as "MF/UF", "NF/RO", "GAC", "Reservoir", or "SDS". It should be noted that samples from the bench-scale reservoirs and SDS were taken ~48 hours after collection and chlorination of GAC filtrate (see Section 2.3).

For comparison with results from the SDS, bulk water samples from El Paso's full-scale drinking water distribution system were collected at 12 sampling locations on January 26, 2016. These 12 sampling locations were selected to cover a range of chlorine concentrations. El Paso targets a free chlorine residual of 1.8 mg/L as Cl_2 entering the full-scale distribution system and a

minimum free chlorine residual of 0.5 mg/L as Cl_2 at all sampling locations throughout the city [28]. These 12 sampling locations were serviced by two drinking water treatment facilities that treated surface water. Each facility employed coagulation, flocculation, sedimentation, filtration (granular activated carbon), and disinfection by either free chlorine or chlorine dioxide. Depending on season, water ages in the full-scale distribution system range from <24 hours to >240 hours, with a typical water age of ~48 hours.

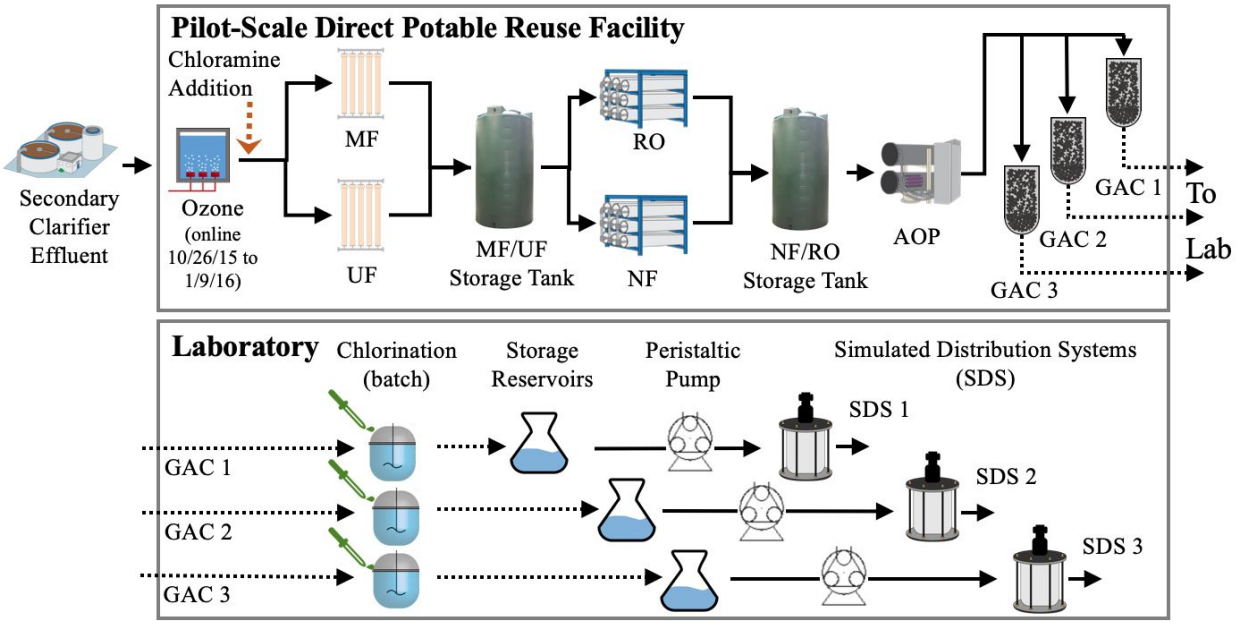

Figure 1: Design of the pilot-scale facility and experimental setup of the simulated chlorination and distribution system. Secondary-treated wastewater was fed to a pilot-scale advanced water treatment train that treated water sequentially using ozonation, parallel microfiltration (MF) and ultrafiltration (UF), parallel nanofiltration (NF) and reverse osmosis (RO), a H_2O_2-UV advanced oxidation process (AOP), and three parallel granular activated carbon (GAC) filters. GAC filtrate was collected, batch chlorinated, stored in reservoirs, and fed into annular reactors that acted as simulated distribution systems (SDS) [9]. Differences in arrow lengths for the laboratory system are purely for visual effect and do not indicate a difference in tubing length or storage times.

Collection of operational data (e.g., MF/UF transmembrane pressure, membrane cleaning and backwash times) and sampling for physical and chemical water quality parameters (including, but not limited to, pH, temperature, total organic carbon, nitrite, total iron and manganese, chloramine, and total ammonia-N {"TAN" = $NH_4^+ + NH_3$}) at various stages throughout treatment were conducted by Arcadis and student researchers from the University of El Paso, Texas. Samples

were dated according to the number of days from pilot start-up (June 8, 2015). We flushed pilot facility sample taps for the following durations prior to collection of bulk water samples: secondary wastewater feed, ozone, and chloramination (>5 min), MF/UF filtrates and storage tank (>15 min), NF/RO permeates and storage tank, and AOP effluent (>30 min), and GAC filtrate (>15 min).

2.2 Annular reactors as simulated distribution systems (SDS): setup and operation

Three biofilm rotating annular reactors (Model 1320 LS; Biosurface Technologies Corporation, Bozeman, MT) were operated as parallel simulated distribution systems (SDS) beginning on October 6, 2015 at the Robertson-Umbenhauer Water Treatment Plant in El Paso, Texas. Annular reactors have been used in many previous studies to simulate drinking water distribution systems [29-32]. Prior to operation, the SDS were sterilized and prepared as described previously [30]. Briefly, storage reservoirs (borosilicate glass), SDS, and associated tubing were sterilized by autoclave, and then 20 ethanol-cleaned polycarbonate biofilm coupons were inserted into each annular reactor. After full assembly, the storage reservoirs and SDS were rinsed by pumping sterile ultrapure water through the systems for ~24 h at the intended operational flow rate. Storage reservoirs and SDS were operated in the dark (i.e., wrapped up tinfoil) at a hydraulic residence time of ~18 hours (flow rate ~0.92 mL/min) and an ambient temperature of 21.5 ± 1.1 ^{o}C. A typical water age in El Paso's full-scale distribution system is ~48 hours (data not shown). However, a lower hydraulic retention time (18 hours) was chosen for the SDS to increase the volume of water that could be collected from the SDS for sequencing analyses, results of which are presented in Kantor et al. (2019) [33]. The inner cylinder rotation speed was set to 50 rpm to create an estimated shear stress of ~0.25 N/m^2 on the inner cylinder surface. This shear stress is reported as common in drinking water pipes in a review of simulation distribution systems by Gomes et al. (2014) [29].

181

182 **2.3 Simulated distribution systems (SDS): collection and chlorination of feed water**

183 Each SDS was fed chlorinated filtrate from a different pilot facility GAC filter. The three GAC
184 filters were acclimated for approximately five months prior to SDS setup. GAC filtrate was
185 collected approximately every two days in 2-L borosilicate glass bottles. Initially, the bottles were
186 cleaned to remove AOC (Hammes and Egli, 2005), then autoclaved and stored in the dark between
187 uses. GAC filtrate was chlorinated to breakpoint at bench-scale with sodium hypochlorite (target
188 CT value of ~30 mg-min/L) and stirred to ensure full and rapid mixing of chlorine. The storage
189 reservoirs were drained of all water and then immediately filled with freshly chlorinated GAC
190 filtrate.

191 The SDS were acclimated for 69 days (pilot operation days 120 – 189) with an average
192 initial feed free chlorine concentration of 0.89 ± 0.07 mg/L as Cl_2. After the acclimation period,
193 the impact of increasing free chlorine concentrations on cell counts and ATP concentrations in the
194 SDS was evaluated by targeting increasingly greater initial free chlorine residuals (in mg/L as Cl_2)
195 in the reservoirs for the following periods of time: 0.8 mg/L (days 189 – 205); 0.9 mg/L (days 206
196 – 214); 1.0 mg/L (days 215 – 228), 1.6 mg/L (days 229 – 234). Free and total chlorine
197 measurements were taken using a DR/850 Portable Colorimeter (Hach USA, Loveland, CO) using
198 DPD 10 mL Free Chlorine (#97009-454; VWR International) and DPD 10 mL Total Chlorine
199 (#97009-464; VWR International, Radnor, PA) Reagent Powder Pillows, respectively.

200 Chlorine demand was calculated by subtracting the initial free chlorine residual
201 concentration (i.e., after achieving a CT value of 30 mg-min/L) measured in the reservoirs from
202 the calculated concentration of chlorine added during chlorination. Ammonia concentration was
203 measured using an online analyzer (ChemScan® UV-6101, ASA Analytics; Waukesha WI) located

after NF/RO. Ammonia in the GAC filtrates was estimated to be the average of five online analyzer measurements (each taken 5 minutes apart), accounting for GAC empty bed contact times, as well as the hydraulic retention times of the NF/RO storage tank and AOP, but assuming negligible losses and transformations of ammonia through storage, AOP [34,35], and GAC. Chlorine demand from ammonia was calculated using a weight ratio of 8:1 (Cl:N) previously reported to achieve complete oxidation of ammonia to nitrogen gas by chlorine [36].

2.4 Cell counts by fluorescent staining and flow cytometry

Total and intact cell counts were measured in triplicate by flow cytometry using slight modifications from a previously optimized protocol presented in Prest et al., 2013 [37]. This modification included pre-heating greater sample volumes (1 mL or 1.5 mL, instead of 500 uL, to account for greater analytical run volumes for low cell count matrices) at 35^{o}C for a longer duration (10 min, instead of 5 min, to account for greater sample volumes). The protocol thereafter followed Prest et al., 2013 [37]. Pre-heated samples were then stained with 10 µL of working dye solution per mL of sample (see below), and then incubated in the dark at 35^{o}C (10 minutes) before measurement by flow cytometry. Working dye solutions for total cell counts were created by diluting SYBR® Green I (10,000x in DMSO, S9430; Sigma-Aldrich, St. Louis, MO) 100x in buffer (10 mM TRIS in 0.1-µm filtered nanopure water); working dye solutions for intact cell counts followed that of total cell counts, but included propidium iodide (30 mM. P1304MP; Life Technologies, Carlsbad, CA) at a working dye concentration of 0.6 mM. Prior to preheating, secondary wastewater, ozonation, and chloramine samples were diluted 10- or 100-fold into syringe-filtered (0.1 µm, Millex-VV® Syringe Filter Unit; Millipore, Billerica, MA) bottled Evian mineral water to achieve final cell counts less than 2 x 10^5 cells/mL.

Sample measurements were performed in technical triplicate (i.e., three measurements taken from the same sample) on an Accuri™ C6 flow cytometer (BD Biosciences, San Jose, CA) equipped with a 50-mW laser emitting a fixed wavelength of 488 nm and volumetric counting software. The cytometer was calibrated (BD Accuri™ Spherotech 6-Peak and 8-Peak Validation Beads; Cat. #653145 and #653144, respectively) according to manufacturer protocol to measure the number of fluorescent particles in a user-defined fluid volume. Bead calibration was performed twice; once prior to any field sampling, and once two months into the sampling campaign. Event counts were triggered on the green fluorescence channel (i.e., FL1) with a threshold of 800 (for FL1-H) [38]. Measurements were performed at a flow rate setting of 66 μL/min. Lower cell count samples (e.g., NF/RO permeate and AOP) were measured with high run volumes (i.e., 1,000 μL) to increase the number of quantified cells. Microbial cell signals were distinguished from background and instrument noise and enumerated on density plots of green (FL1; 533 ± 30 nm) and red (FL3; >670 nm) fluorescence using an electronic gate template previously optimized for water samples [38]. Gate positions for MF, UF, NF, RO, and AOP were modified to reduce the impact of background noise on cell counts (see **Supplementary Figure S1**). The precision of primary measurements is shown in **Supplemental Table S2**.

Calculation of $\log_{10}$ reduction values for cell counts across individual advanced treatment processes were based on process feed and effluent data from each individual sampling day. However, $\log_{10}$ reduction value calculations for the bench-scale reservoir used average data from the GAC filtrates, and calculations for the SDS used average data from the reservoirs. For statistical analyses and $\log_{10}$ removal calculations, all values below the quantification limit were set at the quantification limits (12 and 22 cells/mL for total and intact cell counts, respectively) to reflect the conservative philosophy of drinking water management. Results for cell counts and

ATP were lognormally distributed (all Shapiro-Wilk tests yield $p < 0.05$), and therefore results are presented as geometric means and geometric standard deviations ("geometric SD").

2.5 Adenosine tri-phosphate concentrations

Total and intracellular ATP concentrations were measured in technical triplicate via a previously optimized protocol [17] using BacTiter-Glo™ Microbial Cell Viability Assay reagents (G8231, Promega Corporation, Madison, WI) with a GloMax® 20/20 Luminometer (Turner BioSystems, Sunnyvale, CA). BacTiter-Glo™ reagent was prepared according to manufacturer recommendations, with a >2 hour incubation period of reconstituted reagent at room temperature to diminish background noise. The prepared reagent was then stored at -20 °C and used within 24 hours. Sample analysis, in brief, included simultaneously incubating 500 µL of water sample and 50 µL of prepared reagent in separate tubes at 38 °C for 3 min. Then, 50 µL of the reagent was transferred to the water sample, followed by further incubation at 38 °C for 20 s and then immediate measurement on the luminometer. Luminescence was measured as an integral over 10 s, expressed as relative light units, that were converted to ATP concentrations using an experimentally determined calibration curve (**Supplementary Figure S2**) prepared with a pure ATP standard (P1132; Promega Corporation, Madison, WI). Extracellular ATP was differentiated from total ATP by syringe filtration (0.1 µm, Millex-VV® Syringe Filter Unit; Millipore, Billerica, MA) to remove microbial cells prior to ATP analysis. Intracellular ATP was calculated by subtracting extracellular ATP from total ATP. The accuracy of primary measurements is shown in **Supplemental Table S2**. Samples did not require dilution to remain within the linear range of quantification. Calculation of $\log_{10}$ removal values for ATP followed that of log removal calculations for cell counts. For statistical analyses and $\log_{10}$ removal calculations, all values below

the quantification limit were set at the quantification limit (1 x 10^{-4} nM and 1.82 x 10^{-5} nM for total and intracellular ATP, respectively) to reflect the conservative philosophy of drinking water management.

2.6 Assimilable organic carbon concentrations

AOC-free glassware, filters, and materials were prepared as described previously (Hammes and Egli, 2005). AOC concentrations were determined via batch growth assays in biological triplicate as described previously [25]. Briefly, 50 mL of syringe-filtered (0.22 μm, Millex-GP® Syringe Filter Unit, PES; Millipore, Billerica, MA) water samples were inoculated with 1 mL of unfiltered bottled Evian mineral water to yield initial total cell counts of approximately 1 x 10^4 cells/mL. Previous studies have measured very low concentrations of AOC (i.e., <10 μg/L) in Evian water [39], and use of an Evian microbial inoculum has been shown to obtain similar AOC values in water as using other environmentally-sourced inocula [23]. All samples were supplemented with phosphate, nitrogen, iron, and trace element solution buffers (**Supplementary Table S3)** to create a carbon-limiting environment; nutrient and mineral solution recipes were provided by the Drinking Water Microbiology Group at Eawag, Switzerland [40]. Suspensions were then split into triplicate 20-mL vials via direct pour, and the vials were capped, vortexed, and incubated for 3-5 days at 30°C with continuous gentle shaking. Cell growth was measured by quantifying total cell counts by flow cytometry in technical triplicate at the end of the 3-5 batch period (initial cell counts were assumed to be negligible). AOC concentrations were determined using a conversion factor (9.63 x 10^6 cells per μg of AOC) derived experimentally from growth of Evian microbial inoculum on known acetate concentrations (**Supplementary Figure S3**). All assays were performed with a negative control (a newly purchased bottle of Evian water) that was processed identically to

296 samples. AOC concentrations measured in the negative control were subtracted out from sample
297 results. The accuracy of primary measurements is shown in **Supplemental Table S2**.
298
299 **3. Results and Discussion**
300 **3.1 Cell counts throughout the pilot treatment train**
301 Flow cytometry was a sensitive, rapid, and reproducible method that allowed quantification of
302 planktonic cell concentrations over nearly seven orders of magnitude. All measurements of total
303 and intact cell counts taken throughout the pilot treatment train and three bench-scale SDS are
304 presented in **Figure 2A**, and calculated $\log_{10}$ removal values are presented in **Figure 3A**. Summary
305 statistics and log removal data for cell counts across each treatment process can be found in **Tables**
306 **S5** and **S7,** respectively. The geometric mean total and intact cell counts in the secondary
307 wastewater feed to the pilot were 1.26 x 10^7 cells/mL (geometric SD = 1.95) and 6.31 x 10^6
308 cells/mL (geometric SD = 1.97), respectively. Ozonation reduced total and intact cell counts by an
309 average of 0.20 $\log_{10}$ and 0.91 $\log_{10}$, changes that were not significant ($p = 0.79$ and 0.38,
310 respectively). These relatively low removal values by ozone were unsurprising, given the relatively
311 low initial target ozone concentration of 3.5 mg/L and presumably high demand exerted by
312 organics in the secondary wastewater feed (total organic carbon = 9.3 ± 1.7 mg/L). It should be
313 noted that the primary purpose of ozonation in the El Paso pilot was not to inactivate
314 microorganisms, but to possibly improve the performance and operation of MF/UF membranes.
315 The MF/UF processes provided the greatest average reduction of cells of any treatment
316 process, reducing total and intact cell counts by a combined average of 4.60 and 4.28 $\log_{10}$,
317 respectively. Geometric mean total and intact cell counts in the MF/UF effluent were 2.09 x 10^2
318 cells/mL (geometric SD = 5.33) and 1.12 x 10^2 cells/mL (geometric SD = 5.13), respectively.

These large removal values for cell counts across MF/UF were expected, because the MF and UF membranes had nominal pore sizes of 0.1 μm and 0.04 μm, respectively, which are considerably smaller than the typical size range of 0.3 – 3 μm for wastewater bacteria [41]. The UF achieved greater log removal than MF for both total (4.97 $\log_{10}$ vs. 4.18 $\log_{10}$; $p = 0.046$) and intact cell counts (4.83 $\log_{10}$ vs. 3.67 $\log_{10}$; $p = 0.040$), possibly due to the smaller nominal pore size of the UF membranes.

Cells observed in the MF/UF effluent may be a combination of organisms that passed through MF/UF and organisms that originated from biofilms on the backside of the membranes or other downstream surfaces. Cells can pass through MF/UF via abnormalities in the membranes (e.g., enlarged pores or surface defects) caused by manufacturing imperfections and operational stresses [42], especially if they are members of the "ultra-small" class of bacteria (<0.2 μm) [43]. There were no apparent visual differences in the side and forward scatter cytometric fingerprints of the MF/UF feed and effluent streams that might have indicated substantial passage of small bacteria through the membranes (data not shown).

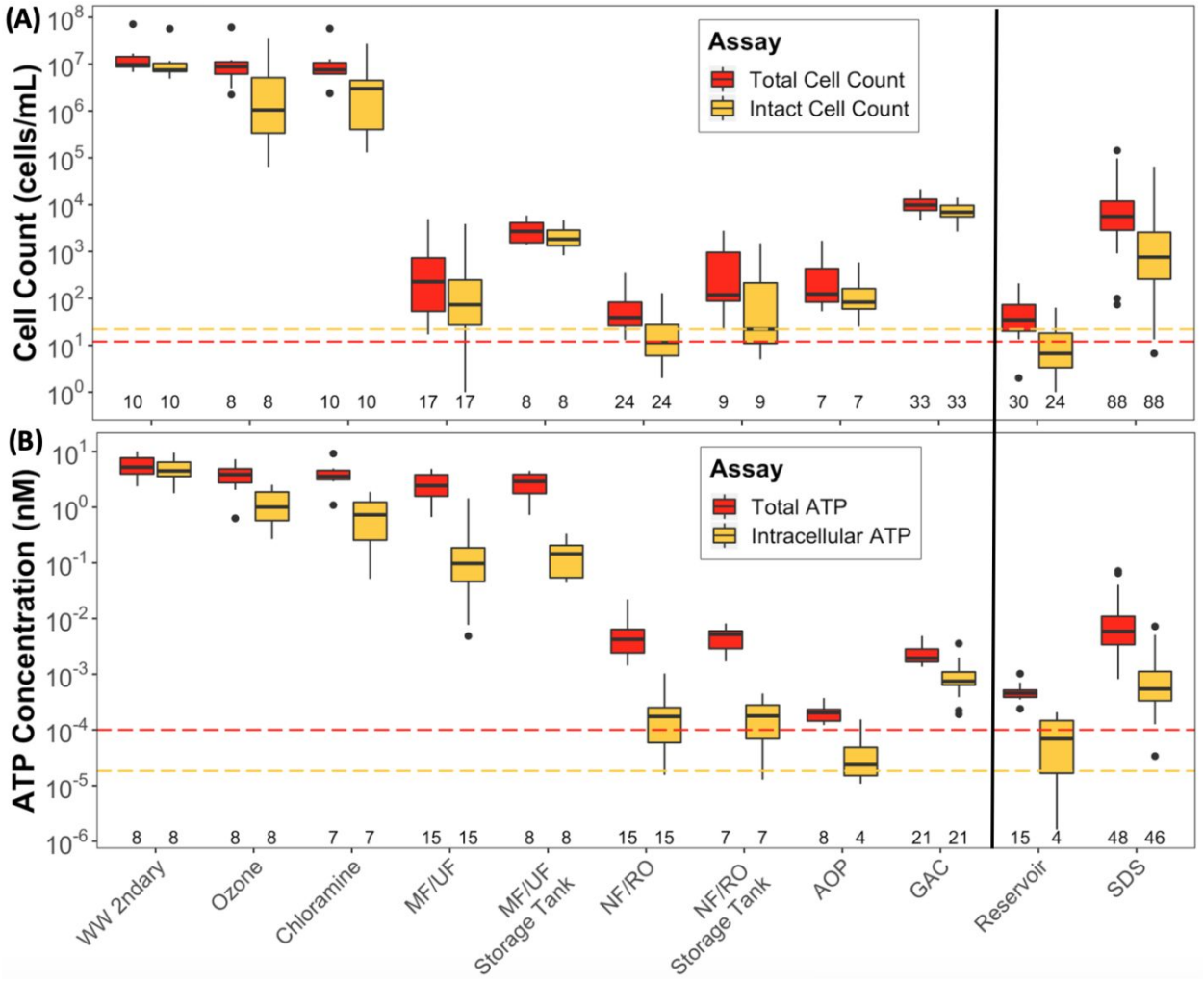

Figure 2. Boxplot of (A) cell counts and (B) ATP concentrations across the pilot facility and into the bench-scale reservoirs and SDS. Data shown for MF/UF, NF/RO, GAC, Reservoir, and SDS are combined measurements from the respective parallel treatment process effluents. The vertical black line indicates batch chlorination of GAC filtrate. The lower limits of quantification for total and intact cell counts (12 and 22 cells/mL) and total and intracellular ATP (1×10^{-4} and 1.82×10^{-5} nM) are indicated by the red and blue colored lines, respectively. The total number of samples taken (n) at each location is located immediately above the x-axes. All samples were analyzed in technical triplicate.

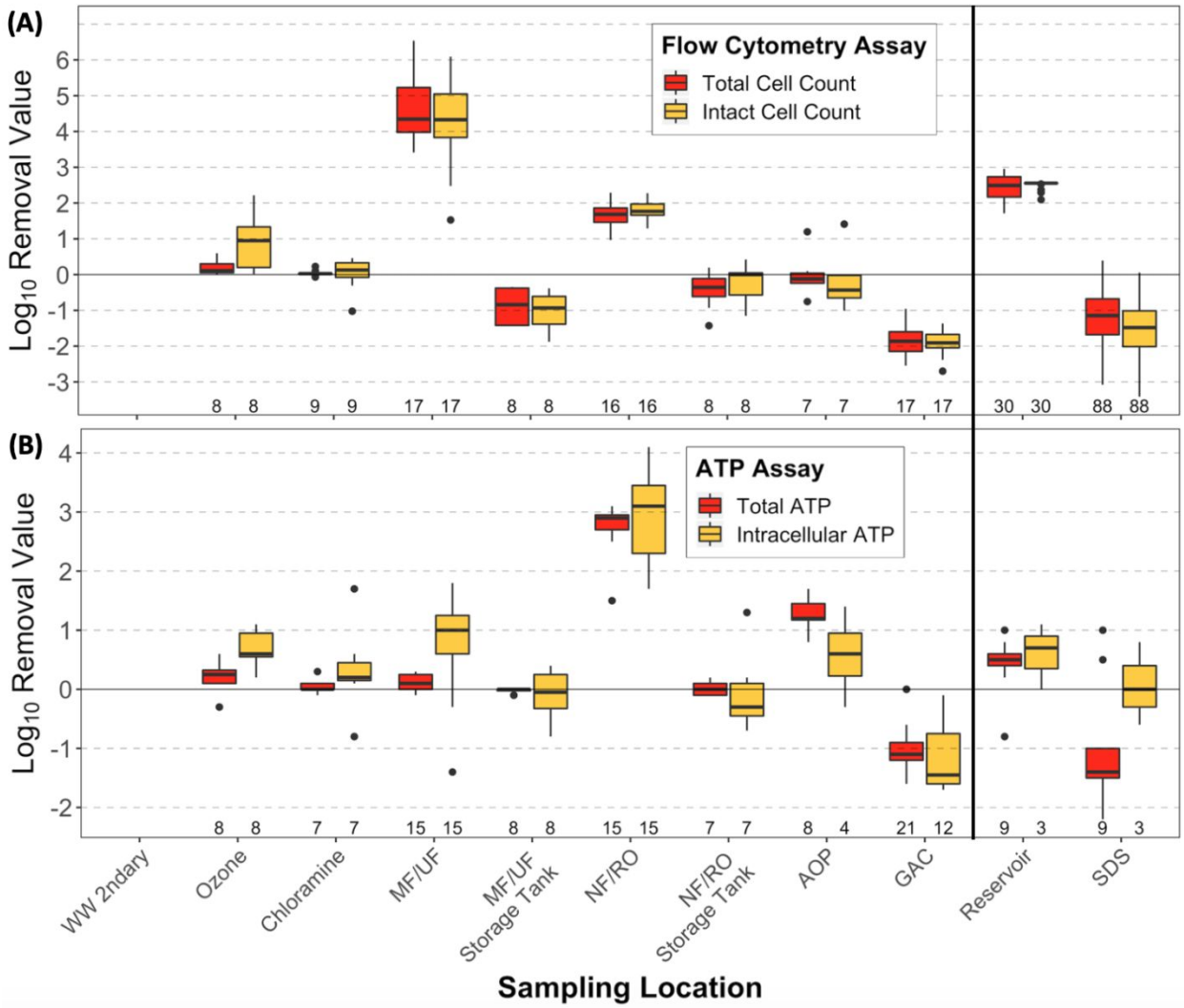

Figure 3. Boxplots of log_{10} removal values for (A) cell counts and (B) ATP concentrations across the pilot facility and into the bench-scale reservoirs and SDS. Data shown for MF/UF, NF/RO, GAC, Reservoir, and SDS are combined measurements from parallel units. The vertical black line indicates batch chlorination of GAC filtrate. The total number of samples taken (n) at each location is located immediately above the x-axes.

Total and intact cell counts rose in the MF/UF effluent storage tank by an average of 0.88 and 1.08 log_{10}, respectively, and then fell by 1.67 log_{10} and 1.80 log_{10} across NF/RO. Geometric mean total and intact cell counts in the NF/RO permeate were 48 cells/mL (geometric SD = 2.44) and 28 cells/mL (geometric SD = 1.66), respectively. Differences in removal of total ($p = 0.272$) and intact cell counts ($p = 0.254$) by NF and RO were not significant. Previous challenge studies of RO membranes have yielded removal values for bacteria of 2.9 to 5.4 log_{10} [42]. However,

assessment of the actual removal capacity of RO/NF was not possible because 71% of intact cell count measurements (n = 24) were below the method quantification limit. Total and intact cell counts increased by an average of 0.45 and 0.13 $\log_{10}$, respectively, between NF/RO permeates and the NF/RO permeate storage tank. Total and intact cell counts rose by 0.01 and 0.20 $\log_{10}$, respectively, through the AOP, but these changes were not significant ($p = 0.39$ and 0.25, respectively). Wünsch et al. (2019) reported a slight but significant decrease in intact cell counts in river water that was subjected to a UV-H_2O_2 AOP (treatment conditions: 4 mg/L H_2O_2 with 600 mJ/cm^2 low pressure UV light) [44]. Regardless, damage to cellular membranes in UV-H_2O_2 AOPs has been shown to be minimal as compared to the inactivation achieved via direct photolysis to genomic DNA (e.g., formation of pyrimidine dimers and adducts) by UV light; this type of damage will not be detected by an intact cell count assay [44,45].

Total and intact cell counts increased by an average of 1.80 and 1.91 $\log_{10}$, respectively, across the GAC filter

s, indicating that a microbial community grew on the filter media that provided a consistent source of cells to the filtrate. There were no significant differences in the change of total or intact cell counts between the three GAC filters ($p > 0.05$ for all comparisons). Microbial growth on the GAC filters may have reached steady-state, based on low variability in the total and intact cell counts (geometric SD = 1.53 and 1.58, respectively) in the GAC filtrate across the pilot sampling period (days 140 – 227). Additionally, we observed consistent microbial community profiles of the GAC filtrates for days 184 – 224 of plant operation based on 16S rRNA gene sequencing results [9]. It is highly unlikely that the major community members originated with the GAC when it was installed. GAC media is produced using very high temperatures ($T >> 100$ ^oC) and stored dry. Cells in the GAC filtrate were most likely from a microbial community that colonized and

continuously multiplied in the GAC media. Subsequent batch chlorination and storage in the reservoir reduced total and intact cell counts by greater than 2.44 and 2.51 $\log_{10}$, respectively, given that 80% of intact cell count measurements were below the quantification limit (n = 30).

Concerns exist that media filters in water treatment facilities might harbor and release opportunistic pathogens, with previous studies reporting increases of *Legionella* spp. [9,46,47] and nontuberculosis mycobacteria [48,49] through sand and GAC filters. However, the methods employed in these papers didn't distinguish between pathogenic and non-pathogenic strains of *Legionella* and mycobacteria, and concentrations of *Legionella* spp. and *Mycobacterium* spp. in the pilot's GAC filtrate was previously reported to be similar to other values reported for conventional drinking water systems [9]. Furthermore, the combination of GAC filtration and chlorination is very similar to what is practiced in conventional drinking water treatment. A recent study by Cheswick et al. (2019) evaluated full-scale chlorination in numerous drinking water treatment facilities and identified a CT value of >30 mg-min/L as a critical threshold for reducing the proportion of intact cell counts to less than 1% [50]. We targeted a CT value of ~30 mg-min/L in bench-scale chlorination; however, we did not measure cell count counts immediately after chlorination (all measurements from the bench-scale storage reservoirs were taken after two days of retention time).

The application of flow cytometry to advanced water treatment necessitated the development of lower method quantification limits. Previous studies have reported quantification limits of ~2 x 10^2 to 1 x 10^3 cells/mL, which would usually permit satisfactory evaluation of drinking water distribution systems, but restricts assessment of treatment processes like MF/UF, NF/RO, AOP, and chlorination [20,26]. Therefore, lower quantification limits for total and intact cell counts were established for low-cell count matrices by using modified electronic gates (see

Figure S1), increasing the sample run volume from 50 to 1,000 µL, and evaluating cell counts from repeated measurements (11x) of un-stained and stained blanks (0.1 µm-filtered bottled mineral Evian water). We set the lower limits of quantification as $\sum(average\ and\ 3 * standard\ deviation)$ of the stained blanks, yielding 12 and 22 cells/mL for the total and intact cell count assays, respectively (**Supplementary Table S4**) [51]. Despite low quantification limits, we observed substantial fractions of intact cell count measurements below the quantification limit after MF/UF, NF/RO, and chlorination (i.e., in the simulated reservoir) (**Supplementary Table S6**).

3.2 Adenosine triphosphate concentrations throughout the pilot treatment train

Similar to flow cytometry, measurement of ATP concentrations has been promoted as a rapid, cultivation-independent alternative to quantify and assess microbial biomass and viability in engineered water systems. In this study, ATP measurement was found to be less sensitive than flow cytometry for detecting changes in microbial biomass through MF/UF and storage tanks, but more sensitive for NF/RO and AOP. All measurements of total and intracellular ATP concentrations taken throughout the pilot treatment train and three bench-scale SDS are presented in **Figure 2B**, and calculated $\log_{10}$ removal values are presented in **Figure 3B**. Summary statistics and log removal data for ATP across all treatment processes can be found in **Tables S6** and **S8**. Geometric mean total and intracellular ATP concentrations in the secondary wastewater feed were 0.727 (geometric SD = 1.62) and 0.663 nM (geometric SD = 1.69), respectively. Extracellular ATP constituted 13% of total ATP in the pilot feed, and this ratio increased to 57% after ozonation and to 75% after chloramination, indicating release of intracellular ATP by oxidative destruction of microbial cells that is consistent with modest decreases in intact cell counts.

MF/UF reduced total and intracellular ATP by an average of 0.11 and 0.79 $\log_{10}$, respectively. These log reductions determined by ATP are ~3 – 4 $\log_{10}$ lower than those determined by flow cytometry. The low reductions in intracellular ATP across MF/UF can be partially ascribed to difficulty in measuring changes in intracellular ATP in water samples with high ratios of extracellular-to-total ATP concentrations (90% for MF/UF) that confound the calculation of intracellular ATP values (intracellular = total – extracellular), a challenge noted previously by a study of ATP concentrations through ozonation and UF treatment of drinking water [20]. There were no statistically significant differences in the removal of total ($p = 0.624$) and intracellular ATP ($p = 0.904$) between the MF and UF membranes.

The average log removal values for total and intracellular ATP through NF/RO (2.76 and 2.92 $\log_{10}$, respectively) were significantly greater ($p < 0.001$) than removal values for total and intact cell counts by ~1 $\log_{10}$. There were no statistically significant differences in the removal of total ($p = 0.834$) and intracellular ATP ($p = 0.834$) between the NF and RO membranes. Significant destruction of total ATP (1.28 $\log_{10}$; $p = 0.002$) was observed across AOP, whereas no significant changes were observed for intracellular ATP (0.58 $\log_{10}$, $p = 0.07$) or cell counts by flow cytometry. Removal of total ATP was likely achieved via reactions with hydroxyl radicals and other oxidants; a previous study reported insignificant changes in ATP concentrations by UV photolysis alone [52].

3.3 Assimilable organic carbon throughout the pilot treatment train

Despite high concentrations of AOC in the secondary treated wastewater feed, the GAC filtrate contained AOC concentrations (average = 66 μg/L) on the lower end of what has been reported in drinking water in the United States [53]. The ozone process was operated from October 26, 2015

– January 9, 2016 to evaluate potential benefits to MF/UF operation and was found to impact AOC concentrations across the treatment train; therefore, changes in AOC across treatment processes were analyzed separately for days when ozone was online versus offline (**Figure 4**). AOC data for all individual processes are available in the supplementary information (**Supplementary Table S9**). AOC concentrations presented herein are the values obtained after subtracting measurements in respective negative controls (mean growth in negative controls = 14 ± 2.5 μg/L; n = 8). Furthermore, for each sampling day, percent changes in AOC across treatment process (e.g., removal efficiencies) were calculated only if influent and effluent data for the respective treatment process were available. AOC in the secondary wastewater was stable over the study period and did not differ significantly ($p = 0.835$) between days the ozone unit was online (327 ± 86 μg/L; n = 5) or offline (342 ± 127 μg/L; n = 5); therefore, differences in subsequent measurements between dates when ozonation did or did not occur were likely not the result of unexpectedly high differences in pilot feed AOC between those dates. The relatively low target ozone concentration of 3.5 mg/L increased AOC by 276 ± 157%, yielding fluctuating post-ozone AOC concentrations with an average of 891 ± 485 μg/L (n = 5). The influence of chloramination (target concentration 2 – 4 mg/L) may have depended on whether the upstream ozone process was in operation. When ozone was offline, chloramination increased AOC by 35 ± 50% (n = 5). However, only one chloramine sample taken when ozone was online passed QA/QC, in which chloramination increased AOC by only 5%. More sampling is required to determine the impact of chloramination on AOC in advanced water treatment.

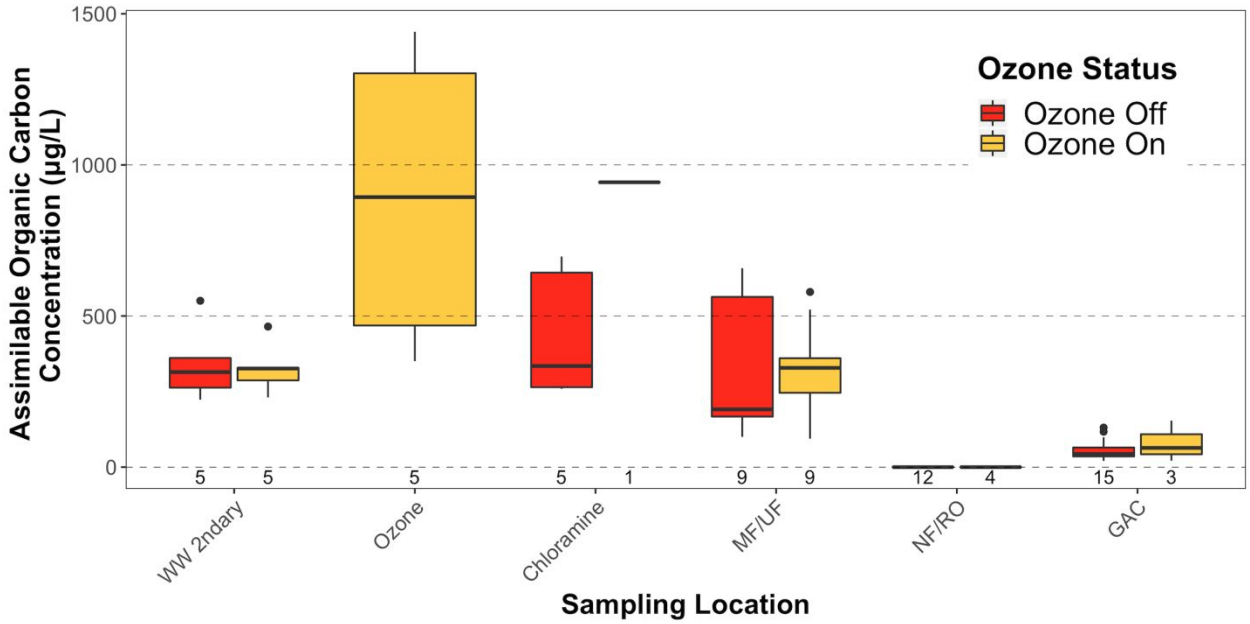

Figure 4: Boxplot of AOC concentrations throughout the pilot treatment facility. MF/UF, NF/RO, and GAC represent combined data from respective parallel treatment process effluents. The total number of samples taken (n) at each location is located immediately above the x-axes. All samples were analyzed in technical triplicate, and data shown are results after subtracting out results from negative controls.

AOC rejection by MF and UF was low immediately following a maintenance clean or recovery clean and increased with time after membrane cleanings (**Figure 5**), a phenomenon discussed further below. Considering all samples taken over the study period, MF and UF were not significantly different in AOC reduction ($p = 0.229$), with AOC reductions of 35 ± 23% for MF ($n = 8$) and 51 ± 32% for UF ($n = 10$). However, considering only samples taken 9 hours or more after membrane cleanings, the measured AOC removal efficiencies for MF and UF were 51 ± 10% ($n = 5$) and 70 ± 14% ($n = 7$), respectively, resulting in a significantly higher removal efficiency for UF as compared to MF ($p = 0.018$). These removal efficiencies for AOC fall within the range of reported total organic carbon rejection efficiencies for MF and UF of 45 – 65% and 50 – 75%, respectively [54]. Furthermore, considering only samples taken 9 hours or more after membrane cleanings, we observed that combined MF/UF AOC concentrations were significantly

higher ($p = 0.043$) when the ozone unit was online (323 ± 172 μg/L; $n = 8$) as compared to offline (156 ± 39 μg/L; $n = 4$).

The MF and UF units underwent maintenance cleans (to reverse moderate fouling) approximately every 48 and 36 hours, respectively, and recovery cleans (to reverse heavy fouling) about once per month (**Figure 5**). MF/UF rejection efficiencies for AOC were $8.8 \pm 6.4\%$ ($n = 6$) when measured between hours 0 and 9 after a membrane cleaning, but rejection efficiencies rose to $62 \pm 15\%$ ($n = 12$) when measured 9 hours or more after a cleaning. Fouling of the MF/UF membranes (as indicated by increases in transmembrane pressures between cleanings; data not shown) resulted in greater rejection efficiencies of AOC. These results are consistent with previous studies of MF and UF that report increasing rejection efficiencies for natural organic matter and dissolved organic carbon as membranes foul via pore plugging, pore size reduction, and cake formation [55,56].

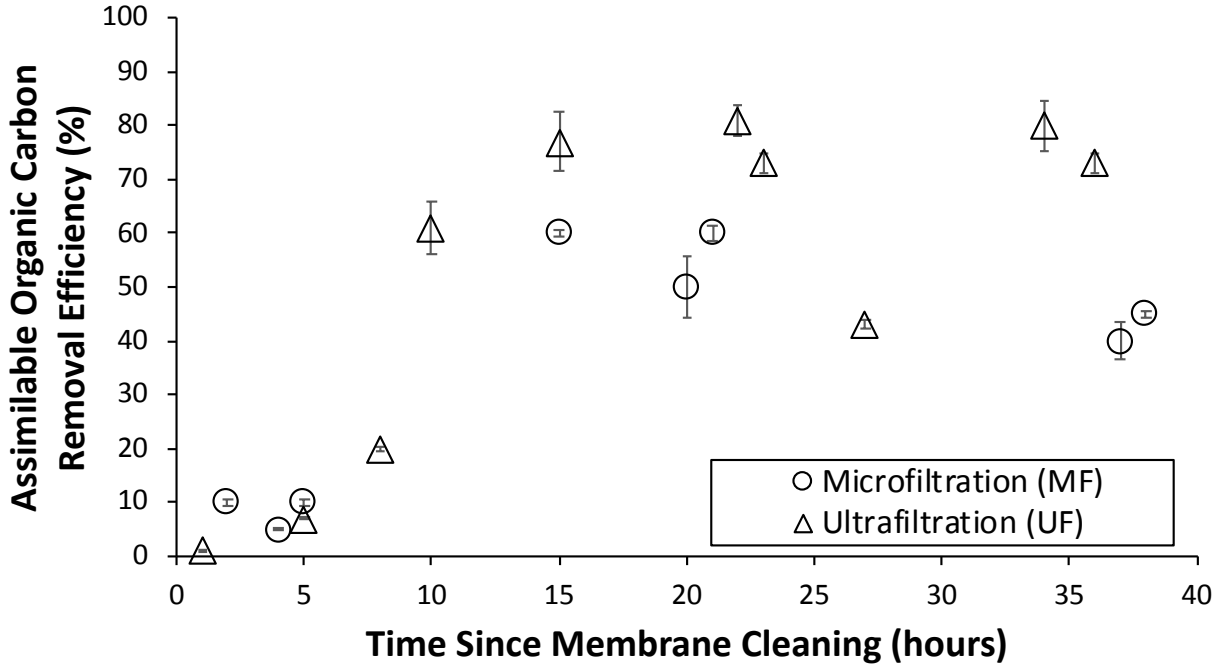

Figure 5: Impact of time since membrane cleanings on the removal efficiency of assimilable organic carbon by MF and UF. All samples were analyzed in technical triplicate. Error bars show standard error of the mean.

As discussed previously, total and intact cell counts rose by 1.10 and 1.62 $\log_{10}$ in the MF/UF storage tank, which were likely driven by high concentrations of AOC in the MF/UF effluents and a 30-min hydraulic retention time in the storage tank. Assuming ~1 μg/L of AOC yields ~10^7 cells/L [57], we estimate that the substantial regrowth observed in the MF/UF storage tank would only have required ~0.25 μg/L. Furthermore, constituents of AOC have not been reported as direct causes of fouling, but rather they serve as a substrate for growth of microorganism that could cause significant biofouling over time [58,59]. Because planktonic bacteria in RO feed waters have been shown to colonize and proliferate across membrane surfaces [60], it may be advantageous to minimize the hydraulic retention time of inter-process storage tanks to limit the numbers of bacteria that regrow in RO feed streams and could contribute to fouling.

All AOC measurements of the NF/RO permeate samples yielded negative results (i.e., after subtracting out results for the negative controls), which suggests growth inhibition of the Evian inoculum in NF/RO permeate. Growth inhibition was likely not due to nutrient limitations, because all AOC assays were amended with nutrient buffers containing 14 macro- and micronutrients (e.g., P, N, S, Fe, Mn, Co, etc.) previously designed to force carbon limitation [61]. Rather, growth was likely inhibited in NF/RO permeate samples by low pH (~5.3 – 5.5) that can hinder transport of compounds across cellular membranes [62] and force bacteria to expend excess energy to maintain homeostasis [63]. A recent study of bacterial growth methods by Sousi et al. (2018) reported inhibition of growth in RO samples at low pH (5.5) but significant growth following adjustment of RO sample pH to 7.8 with a sodium bicarbonate solution [64]. Future studies applying microbial regrowth methods to measure AOC in NF and RO permeates should explore adjustment of sample pH in addition to mineral and nutrient amendments to overcome possible growth inhibition.

524 The average AOC concentration in the GAC filtrate was 60 ± 37 μg/L. Filtrate AOC
525 concentrations for GAC 1 were 67 ± 55 μg/L and for GAC 2 were 66 ± 35 μg/L. GAC 3 had lower
526 filtrate AOC concentrations (47 ± 26 μg/L) than GAC filters 1 or 2, which could be due to the
527 longer empty bed contact time (15 min vs. 5 min, respectively), but this difference in filtrate AOC
528 was not significant ($p = 0.257$). Sources of AOC in the GAC filtrates may have been partially
529 composed of low molecular weight, uncharged carbon compounds (e.g., alcohols and aldehydes)
530 that passed through RO but were below the AOC method detection limit (possibly due to inhibition
531 by low pH) at the NF/RO sampling location [65]. This possibility is supported by metagenomes
532 recovered from the GAC media-associated biofilm and filtrates, in which genes associated with
533 the metabolisms of methanol and formaldehyde were identified [9]. If RO permeate was a source,
534 we would expect higher AOC in the GAC filtrate when ozonation was online (80 ± 68 μg/L; $n =$
535 3) versus offline (56 ± 33 μg/L; $n = 15$), a trend that was observed but was not statistically
536 significant ($p = 0.613$). Another potential source of carbon was autotrophic production by algae,
537 consistent with observations of green growth on the walls of the uncovered GAC media columns
538 and metagenomic detection of genes in the GAC media-associated biofilm likely corresponding to
539 the green algal order Sphaeropleales [9]. A final potential carbon source may have the GAC media
540 itself, but to our knowledge the leaching of labile carbon from GAC media has not been reported
541 in the literature.

542 The average measured AOC concentration of 66 μg/L in the GAC filtrates is on the lower
543 end of values previously reported in treated and distributed drinking waters in the United States.
544 A study of 95 drinking water treatment facilities by Volk and LeChevallier (2000) reported average
545 treated effluent AOC concentrations of ~100 μg/L, with only 9% of facilities producing a treated
546 effluent with AOC <50 μg/L [53]. The El Paso pilot facility produces a finished water (i.e., GAC

547 filtrate) more similar to that reported for drinking water treatment in Zürich, Switzerland (32 μg/L)
548 [25] and Rotterdam, the Netherlands (~30 μg/L) [18]. These treatment systems employ ozonation
549 followed by biological filtration to reduce concentrations of labile carbon and maintain biological
550 stability in the distribution system without the application of a residual disinfectant.
551
552 **3.4 Microbial abundance dynamics in the simulated distribution systems (SDS)**
553 Residual free chlorine exhibited a strong influence on planktonic cells in the SDS, in which
554 we observed a clear inverse correlation for both total and intact cell counts with free chlorine
555 concentrations (**Figure 6**). Increasing free chlorine residual was expected to lower cell counts,
556 given previous reports of lower heterotrophic plant counts and total coliforms at higher chlorine
557 residual concentrations in distribution systems [7,66,67]. Measurements of flow cytometric cell
558 counts and free chlorine residual from the three SDS indicate that an inverse relationship also
559 exists between the entire population of planktonic cells and free chlorine, a finding that is
560 consistent with studies of full-scale drinking water distribution systems in Scotland [51], Latvia
561 [19], and France [68]. However, this is the first demonstration of cell counts and chlorine dynamics
562 in the distribution of advanced treated water, for which we expect the relatively lower suspended
563 solids and organic matter content to increase disinfection efficacy (relative to conventionally-
564 sourced drinking water) by reducing protection afforded to microorganisms [69]. Several other
565 parameters have been linked to planktonic cell concentrations in distribution systems, such as
566 temperature [18,70], water age [19,71,72], concentrations of labile carbon [6,18,73], and
567 concentrations of nutrients [74,75], but we did not test for these relationships.

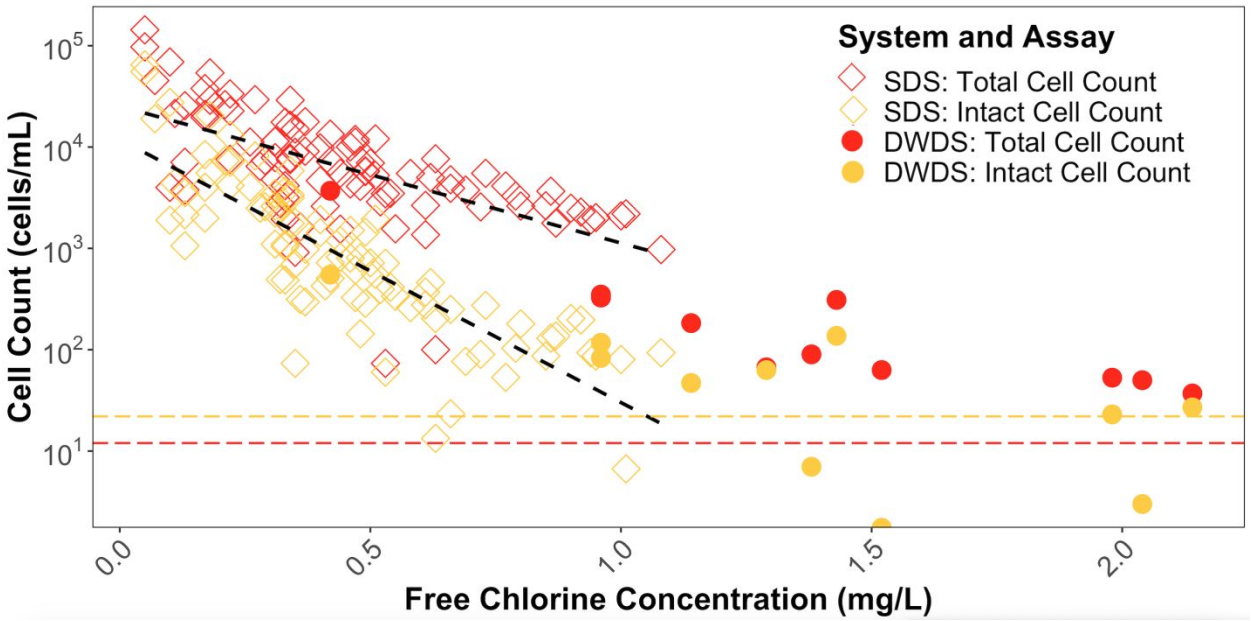

Figure 6: Effect of free chlorine concentration on total and intact cell counts in the SDS and in El Paso's full-scale drinking water distribution system (DWDS). Regression models (dashed blank lines) were developed from cell counts in the SDS only. SDS data only includes samples taken after the SDS acclimation period (i.e., after Day 189 of pilot operation). The limits of quantification for total and intact cell counts (12 and 22 cells/mL) are indicated by the dashed red and blue colored lines, respectively. All samples were analyzed in technical triplicate.

The inverse relationship of cell counts and free chlorine concentration in the SDS may be stronger than in typical full-scale distribution systems due to enhanced free chlorine disinfection conditions prior to, and in the SDS (i.e., relatively low pH and efficient mixing), less established biofilms, and lower amounts of suspended solids and loose deposits that can harbor microorganisms [76]. The average pH of the NF and RO permeates was 5.61 and 5.71, respectively, which rose to 6.53 ± 0.18 in the SDS (n = 204) without adjustment, and is lower than the typical pH range of 7.3 – 8.1 for El Paso's full-scale distribution system [77]. Because free chlorine is a weak acid ($HOCl/OCl^-$, $pK_A = 7.54$), at a pH of 6.53 about 90% of the SDS chlorine residual would have existed in the form of HOCl, which is estimated to be 40-80x more effective at inactivating bacteria than its counterion OCl^- [78,79]. It should be noted that for full-scale membrane-based potable reuse facilities, the lack of minerals and low pH of NF/RO permeates will necessitate pH adjustment and remineralization (e.g., decarbonation and lime addition) of

finished water to limit corrosion of distribution infrastructure [80]. Therefore, the lack of pH adjustment and remineralization of GAC filtrate in this study somewhat limits the applicability of the SDS results to full-scale potable reuse systems.

Free chlorine exerted more influence on intact cell counts than total cell counts, as evidenced by log-linear slopes of -1.50 ± 0.13 for total cell counts (R^2 = 0.675, n = 68) and -2.71 ± 0.17 for intact cell counts (R^2 = 0.787, n = 68) (**Figure 6**). This greater decline in intact cell counts with increasing free chlorine residual may be attributable to more widespread oxidative damage to cellular membranes without complete destruction of cells, a finding previously observed during free chlorine disinfection [81]. We were unable to find regression models in the literature for other simulated or full-scale drinking water distribution systems.

The relationship between cell counts in the SDS and free chlorine residual can also be visualized as a time series (**Supplementary Figure S4).** Significant decay of the free chlorine residual occurred in the SDS, as measured by large differences in free chlorine (59 ± 16%, n = 102) between the reservoirs and the SDS. In general, total and intact cell counts rose as the free chlorine residual fell in the SDS, and vice versa. Throughout the study, the storage reservoirs contained high concentrations of free chlorine (>0.5 mg/L as Cl_2) and low geometric mean total (39 cells/mL; geometric SD = 2.18) and intact cell counts (24 cells/mL; geometric SD = 1.28). Despite a low inflow of planktonic cells, the SDS harbored large quantities of total and intact cells, likely due to a combination of bulk water regrowth and release of cells from tubing and reactor surface biofilms. A recently published study of a full-scale system fed with ultrafiltered (i.e., low-cell count) drinking water estimated that >50% of planktonic cells in distribution originated from pipe biofilm (the remaining fraction originated from the treatment facility's finished water), but the researchers assumed negligible regrowth of bacteria in the bulk water due to short residence

611 times (<25 hour) and low temperatures (~7.5 °C) [82]. However, the higher temperatures (~21.5
612 °C) in the SDS described here could be more conducive to microbial growth.

613 Twelve samples were collected from El Paso's drinking water distribution system on
614 January 26, 2015 for comparison to the SDS results (**Figure 6**). These samples had an average free
615 chlorine concentration of 1.4 mg/L as Cl_2 (range: 0.42 – 2.14 mg/L), pH of 7.9 ± 0.2, and
616 temperature of 20.6 ± 0.25 °C. It is difficult to draw comparisons between the full-scale and
617 simulated systems given substantial differences in residual free chlorine and the limited number
618 of full-scale samples. It should be noted that the target free chlorine residual (~1.0 mg/L as Cl_2)
619 for the SDSs was chosen to increase total biomass available (compared to higher residual
620 concentrations) for 16S ribosomal and metagenomic sequencing analyses; these results were
621 published separately [9].

622 Previous studies have calculated ATP content per cell ("ATP-per-cell") to assess changes
623 in metabolic activity [83,84] and to propose conversion factors for estimating bacterial cell
624 concentrations from ATP data [17,21,85]. It is crucial for researchers to note the specific
625 methodology used for calculating ATP-per-cell, because results will vary depending on use of total
626 or intracellular ATP, viable or total cell counts, and cell units or cell biovolume. A correlation (R^2
627 = 0.47; $p < 0.001$; n = 43) was observed between intracellular ATP and intact cell count
628 measurements in the SDS (**Supplementary Figure S5**), resulting in a geometric mean ATP-per-
629 cell value of 5.50×10^{-10} nmol/cell (geometric SD = 3.23; n = 43), which is about 4.5 times greater
630 than the geometric mean 1.23×10^{-10} nmol/cell (geometric SD = 2.12; n = 21) found in the GAC
631 filtrates from this study, and about three times greater than the average 1.74×10^{-10} nmol/cell
632 reported previously by Hammes et al. (2010) [17]. Interestingly, Hammes et al. (2010) tested many
633 water types (i.e., groundwater, lake and river water, bottled water, unchlorinated drinking water,

634 wastewater effluent) and found their ATP-per-cell value applied to all tested waters; however, their
635 dataset did not include chlorinated drinking water. ATP-per-cell values can be influenced by the
636 physiological state, size, and composition of microorganisms in a sample [17,83,84,86], all of
637 which in turn can be influenced by the presence of chlorine [87-89]. Considering that the GAC
638 filtrate and SDS shared a large portion of their microbial communities, we speculate that the
639 presence of a free chlorine residual in the SDS elevated the average metabolic activity of
640 microorganisms as compared to the GAC filtrate.
641
642 **3.5 Dynamics of chlorination and chlorine demand**
643 A high variability in chlorine demand of the GAC filtrates was observed across the study
644 period, which tracked closely with estimated demand from ammonia (**Figure 7)**. Total ammonia-
645 N (TAN) fluctuations in the pilot were linked to diurnal variations in nitrification efficiency in the
646 upstream secondary wastewater treatment facility. The activated sludge treatment process
647 frequently failed to nitrify influent TAN fully during peak loading periods (e.g., mid-morning),
648 leading to average and 90th percentile concentrations of TAN in the pilot feed of 3.0 and 7.5 mg/L
649 as N, respectively (n = 54,592). The NF/RO membranes were expected to achieve the majority of
650 TAN removal. Because sulfuric acid addition in the NF/RO feed dropped the pH to ~6.5 to limit
651 mineral scaling on the membrane, the vast majority of TAN likely existed in the form of
652 ammonium (pKa = 9.24), which has previously reported rejection efficiencies by RO of >95%
653 [90]. Despite a cumulative removal efficiencies of ~93% for TAN through NF/RO, the average
654 and 90th percentile concentrations of TAN in the RO permeate were 0.20 and 0.40 mg/L as N,
655 respectively (n = 47,394), although 71% of measurements were below the method detection limit
656 (0.1 mg/L as N). However, the average TAN concentration in the NF/RO permeate rises to 0.37 ±

0.35 mg/L as N when considering only days for which measurements of TAN in the NF/RO permeate were above the detection limit. TAN would likely pass through the AOP and GAC filters and ultimately cause an estimated chlorine demand of 3.0 ± 2.8 mg/L during breakpoint chlorination of GAC filtrate, assuming a 8:1 weight ratio of Cl:N [36]. Zeng et al. (2015) observed higher TAN concentrations in the finished water from five potable reuse advanced treatment trains (range: 0.19 – 2.41 mg/L as N), which would exert 1.5 – 19.3 mg/L of chlorine demand [5]. It should be noted that conventional wastewater treatment facilities have been designed and operated to meet specific standards (e.g., environmental protection) that differ from what may be desired for optimal preparation of wastewater for advanced treatment [91].

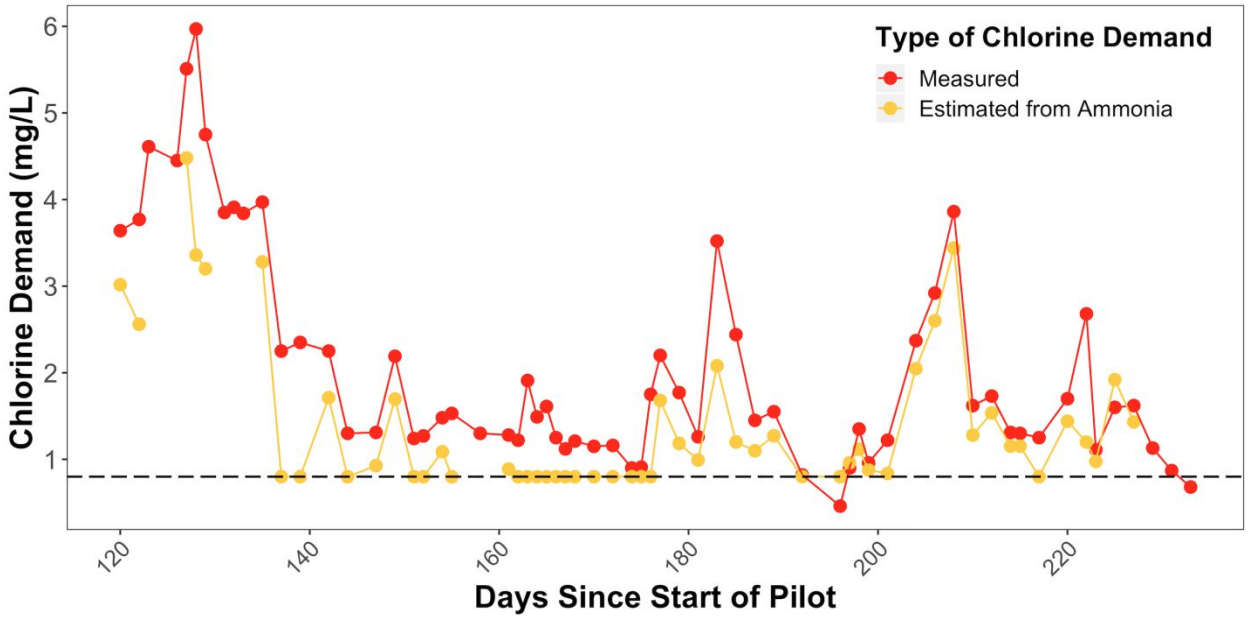

Figure 7: Chlorine demand in bench-scale breakpoint chlorination of the pilot's GAC filtrates. Measured chlorine demand for each day is the average from the three GAC filtrates. The limit of detection for estimated demand from ammonia (based on a 0.1 mg/L limit of detection for measurement of ammonia-N in the NF/RO permeate) is indicated by the horizontal dashed blue line.

Considering all days the GAC filtrate was breakpoint chlorinated, the average measured chlorine demand in GAC filtrate was 2.04 mg/L (median = 1.54 mg/L; n = 192). However, an measured chlorine demand surpassed 3.0 mg/L on 20% of batch chlorination days (n = 64), with

676 a maximum measured chlorine demand of 5.97 mg/L. Neglecting days for which TAN
677 concentrations were below the online analyzer's detection limit (0.1 mg/L as N), we estimated that
678 demand from TAN accounted for an average of 79 ± 15% of measured chlorine demand (n = 34).
679 Other possible sources of chlorine demand in the GAC filtrates included organic material, metals,
680 and nitrite. In the NF/RO permeate grab samples, however, average and 90th percentile
681 concentrations were low and relatively stable for total organic carbon (0.37 and 0.49 mg/L; n =
682 14), nitrite-N (0.04 and 0.06 mg/L; n = 122), total iron, (<0.04 and <0.04 ug/L; n = 14) and total
683 manganese (<2.5 and <3.5 ug/L; n = 14).
684

685 **4. Implications for Practice and Future Research**

686 The combination of flow cytometry with ATP measurements more completely tracked
687 microbial abundance and viability throughout advanced treatment than either method alone,
688 supporting previous studies that have proposed pairing these two cultivation-independent
689 approaches to assess drinking water systems [15-19]. The choice of which method to employ
690 depends on what treatment process is being evaluated. Regarding NF/RO, we observed greater
691 removal values of total ATP (2.71 ± 0.39 $\log_{10}$) as compared to total cell counts by flow cytometry
692 (1.67 ± 0.40 $\log_{10}$). Moreover, credited removal of pathogens by RO membranes is typically based
693 on ambient indicators such as conductivity or total organic carbon, but removal of these
694 compounds by RO is typically low (1 – 2.3 $\log_{10}$) [92] when compared to the removal of pathogens
695 such as adenovirus (2.7 – 6.5 $\log_{10}$) [4]. Measured removal of ambient ATP may be a better
696 indicator for pathogen removal by NF/RO than currently accepted parameters. In contrast to
697 NF/RO, we observed much greater removal of total cell counts (4.60 ± 0.72 $\log_{10}$) as compared to
698 total (0.11 ± 0.14 $\log_{10}$) or intracellular ATP (0.79 ± 0.79 $\log_{10}$) across the MF/UF membranes.

699 Observed removal of cells by flow cytometry was similar to and frequently higher than the 4 $\log_{10}$
700 removal credited for *Cryptosporidium* and *Giardia* by MF/UF pressure decay tests [93]. However,
701 these decay tests are indirect, are typically only conducted once or twice per day, and yield scant
702 information about performance trends that are time-dependent (e.g., effects of membrane cleanings
703 on pathogen removal). Online and continuous measurements of total cells across MF/UF or total
704 ATP across NF/RO could provide enhanced and more accurate monitoring of microbial removal
705 in advanced treatment trains. However, the benefits and drawbacks to full-scale implementation
706 of flow cytometry and ATP analysis must also be compared with other emerging techniques. For
707 example, the IMD-W™ bacteriological counter (BioVigilant, Tuscon, AZ) has recently been used
708 to quantify cells in RO feed and permeate without the use of reagents, which could significantly
709 lower operating costs for continuous quantification of bacteria as compared to stain-intensive flow
710 cytometric methods [94].

711 Continuous flow cytometry has recently been applied for evaluating the microbial water
712 quality of unchlorinated tap water [95,96] and evaluating simulations of shock chlorination [89],
713 but has yet to be applied to advanced treatment trains. Future research is warranted to explore the
714 potential for online, continuous flow cytometry to enhance monitoring of advanced treatment
715 processes, specifically MF/UF, full-scale chlorination, regrowth in inter-process storage tanks, and
716 evaluating the biological activity of GAC filters. More research is also needed to determine the
717 utility of flow cytometry, either with grab samples or on-line configuration, to monitor microbial
718 water quality in both conventional and potable reuse distribution systems.

719 However, application of enhanced microbial evaluation tools also highlighted the
720 continued challenges in microbial monitoring of advanced treated water. For example, although
721 we detected low total and intact cell counts (e.g., <50 cells/mL) in advanced treated and chlorinated

722 water, evaluation of actual removal efficiencies was constrained by the limits of quantification.
723 Furthermore, removal efficiencies of ATP concentrations were low through ozonation and MF/UF
724 as compared to removal observed for cell counts. This is similar to a finding by Hammes et al.
725 (2010), who cautioned the use of ATP measurements in these water treatment matrices [20].
726 Finally, more work is needed to overcome inhibition due to low pH, minerals, and nutrients when
727 applying growth-based bioassays for waters treated by NF or RO. A recent study by Sousi et al.
728 (2018) successfully applied a growth-based bioassay to groundwater treated by RO, but such
729 methods still need to be successfully applied to RO/NF and AOP matrices in potable reuse [64].
730 The large fluctuations in ammonia-based chlorine demand in the finished water (i.e., GAC
731 filtrate) observed in this study highlights one potential challenge of producing purified water with
732 a stable chlorine residual at full-scale facilities. Some advanced treatment facilities rely on free
733 chlorine disinfection for large removal credits for viruses (4 – 6 $\log_{10}$) to meet stringent potable
734 reuse regulations for pathogens [3], which will be more difficult to achieve with fluctuating
735 chlorine demand. Moreover, reducing chlorine demand can minimize the formation of disinfection
736 byproducts (e.g., haloacetonitriles and haloacetaldehydes), which have been observed in higher
737 concentrations following chlorine-based advanced oxidation of NF/RO permeate [97,98]. It should
738 be noted that greater total ammonia-N concentrations have been observed in other studies of
739 advanced treatment trains [99], which would cause considerably greater chlorine demand than that
740 reported herein. Thus, we recommend ensuring complete nitrification upstream in conventional
741 wastewater treatment, which could have additional benefits for advanced treatment by reducing
742 biofouling and operating pressures of MF membranes [100]. Future research is needed to
743 investigate the impacts chemical conditioning of RO and NF permeates (e.g., pH adjustment and
744 remineralization to prevent pipe corrosion) may have on disinfection processes. There also remains

a need to evaluate the efficacy and stability of chlorine residual in potable reuse distribution systems.

Lastly, more research is needed to evaluate the impact of different final treatment steps (e.g., GAC filtration) on finished water quality, as well as characterizing the implications of introducing advanced treated wastewater into existing distributions systems. Although not intended to be operated in biological mode, the GAC filters in this study harbored a microbial community that was both active (as indicated by increases in intact cell counts through filtration) and previously reported to be consistent over time [9]. From a treatment process perspective, a last-stage GAC filter can act as an additional barrier for organic pollutants [101], such as through microbially-mediated breakdown of disinfection byproduct precursors [102], while not increasing concentrations of opportunistic pathogens relative to conventional water systems [9]. From an ecological perspective, a diverse microbial community in distribution should lead to greater biological stability and be more capable of outcompeting frank and opportunistic pathogens [103,104]. Because advanced treatment decreases bacterial presence and diversity, seeding of microbes from GAC filters could increase finished water biostability. In a complementary study of this pilot system we observed some microbial diversity shared between GAC filtrates and the SDS [9], but more research is needed to determine the impacts of final treatment steps on microbial ecology in distribution.

Funding

This work was supported by the National Science Foundation (NSF) through the Engineering Research Center for Reinventing the Nation's Urban Water Infrastructure (ReNUWIt) EEC-

1028968, the Environmental Protection Agency Science to Achieve Results Graduate Fellowship (EPA STAR no. 91782901-0) to S. E. Miller, and El Paso Water.

Acknowledgements

We are deeply grateful to Arcadis NV and El Paso Water for their partnership and generosity in time, labor, and laboratory resources. We thank the pilot's operator Chelsea Merrick for her help in sampling the facility. The authors also thank Dr. Frederick Hammes and Dr. Caitlin Proctor for their mentorship on the assays used herein, as well as Cesar Navar, Lauren Kennedy, and Dr. Rose Kantor for laboratory and data analysis support. We thank Aidan Cecchetti and Dr. Sara Gushgari for manuscript edits, and Emily Marron and Dr. Daniel Daft for use of advanced treatment images.

Publication Disclaimer

This publication was developed under STAR Fellowship Assistance Agreement no. 91782901-0, awarded by the U.S. Environmental Protection Agency (EPA). It has not been formally reviewed by EPA. The views expressed in this publication are solely those of the listed authors, and the EPA does not endorse any products or commercial services mentioned in this publication.

References

1. Maseeh GP, Russell CG, Villalobos SL, Balliew JE, Trejo G. El Paso's Advanced Water Purification Facility: A New Direction in Potable Reuse. J Am Water Works Assoc. 2015 Nov 1;107(11):36–45.

2. Gerrity D, Pecson B, Trussell RS, Trussell RR. Potable reuse treatment trains throughout the world. J Water Supply: Res and Tech [Internet]. IWA Publishing; 2013 Sep 1;62(6):321–38. Available from: https://doi.org/10.2166/aqua.2013.041

3. Pecson BM, Triolo SC, Olivieri S, Chen EC, Pisarenko AN, Yang C-C, Olivieri A, Haas CN, Trussell RS, Trussell RR. Reliability of pathogen control in direct potable reuse:

Performance evaluation and QMRA of a full-scale 1 MGD advanced treatment train. Water Res. Elsevier Ltd; 2017 Oct 1;122:258–68.

4. Soller JA, Eftim SE, Warren I, Nappier SP. Evaluation of microbiological risks associated with direct potable reuse. Micro Risk Anal. Elsevier B.V; 2016 Sep 8;:1–12.

5. Zeng T, Mitch WA. Contribution of N-Nitrosamines and Their Precursors to Domestic Sewage by Greywaters and Blackwaters. Environ Sci Technol. 2015 Nov 17;49(22):13158–67.

6. van der Kooij D. Assimilable Organic Carbon as an Indicator of Bacterial Regrowth. J Am Water Works Assoc [Internet]. 1992 Feb;84(2):57–65. Available from: https://www.jstor.org/stable/41293634

7. LeChevallier MW, Welch NJ, Smith DB. Full-scale studies of factors related to coliform regrowth in drinking water. Appl Environ Microbiol. American Society for Microbiology (ASM); 1996 Jul 1;62(7):2201–11.

8. Thayanukul P, Kurisu F, Kasuga I, Furumai H. Evaluation of microbial regrowth potential by assimilable organic carbon in various reclaimed water and distribution systems. Water Res. Elsevier Ltd; 2013 Jan 1;47(1):225–32.

9. Kantor RS, Miller SE, Nelson KL. The Water Microbiome Through a Pilot Scale Advanced Treatment Facility for Direct Potable Reuse. Front Microbiol. 2019 May 8;10.

10. Stamps BW, Leddy MB, Plumlee MH, Hasan NA, Colwell RR, Spear JR. Characterization of the Microbiome at the World's Largest Potable Water Reuse Facility. Front Microbiol. 2018 Oct 25;9:1–16.

11. Park SK, Hu JY. Assessment of the extent of bacterial growth in reverse osmosis system for improving drinking water quality. Journal of Environmental Science and Health, Part A. 20 ed. 2010 Jun 4;45(8):968–77.

12. Meckes MC, Haught RC, Kelty K, Blannon JC, Cmehil D. Impact on water distribution system biofilm densities from reverse osmosis membrane treatment of supply water. J Env Eng and Sci. 2007 Jul;6(4):449–54.

13. Laurent P, Servais P, Gatel D, Randon G, Bonne P, Cavard J. Microbiological quality before and after nanofiltration. J Am Water Works Assoc. 1999 Oct 1;91(10):62–72.

14. Garner E, Inyang M, Garvey E, Parks J, Glover C, Grimaldi A, Dickenson E, Sutherland J, Salveson A, Edwards MA, Pruden A. Impact of blending for direct potable reuse on premise plumbing microbial ecology and regrowth of opportunistic pathogens and antibiotic resistant bacteria. WR. Elsevier Ltd; 2019 Mar 15;151:75–86.

15. Berney M, Vital M, Hülshoff I, Weilenmann HU, Egli T, Hammes F. Rapid, cultivation-independent assessment of microbial viability in drinking water. Water Res. 2008 Aug;42(14):4010–8.

16. Vital M, Dignum M, Magic-Knezev A, Ross P, Rietveld L, Hammes F. Flow cytometry and adenosine tri-phosphate analysis: Alternative possibilities to evaluate major bacteriological changes in drinking water treatment and distribution systems. WR. Elsevier Ltd; 2012 Oct 1;46(15):4665–76.

17. Hammes F, Goldschmidt F, Vital M, Wang Y, Egli T. Measurement and interpretation of microbial adenosine tri-phosphate (ATP) in aquatic environments. Water Res. Elsevier Ltd; 2010 Jul 1;44(13):3915–23.

18. Prest EI, Vrouwenvelder JS, Van Loosdrecht MCM, Hammes F, Weissbrodt DG. Long-Term Bacterial Dynamics in a Full-Scale Drinking Water Distribution System. Paranhos R, editor. PLoS ONE. 2016 Oct 28;11(10):e0164445–20.

19. Nescerecka A, Rubulis J, Vital M, Juhna T, Hammes F. Biological Instability in a Chlorinated Drinking Water Distribution Network. PLoS ONE. 2014 May 5;9(5):1–11.

20. Hammes F, Berney M, Wang Y, Vital M, Köster O, Egli T. Flow-cytometric total bacterial cell counts as a descriptive microbiological parameter for drinking water treatment processes. Water Res. 2008 Jan;42(1-2):269–77.

21. Siebel E, Wang Y, Hammes F. Correlations between total cell concentration, total adenosine tri-phosphate concentration and heterotrophic plate counts during microbial monitoring of drinking water. Drink Water Eng Sci Discuss. 2008 Jun 2;1:1–6.

22. Van Nevel S, Koetzsch S, Proctor CR, Besmer MD, Prest EI, Vrouwenvelder JS, Knezev A, Boon N, Hammes F. Flow cytometric bacterial cell counts challenge conventional heterotrophic plate counts for routine microbiological drinking water monitoring. WR. Elsevier Ltd; 2017 Apr 15;113:191–206.

23. Hammes FA, Egli T. New Method for Assimilable Organic Carbon Determination Using Flow-Cytometric Enumeration and a Natural Microbial Consortium as Inoculum. Environ Sci Technol. 2005 May;39(9):3289–94.

24. Polanska M, Huysman K, van Keer C. Investigation of assimilable organic carbon (AOC) in flemish drinking water. Water Res. 2005 Jun;39(11):2259–66.

25. Hammes F, Berger C, Köster O, Egli T. Assessing biological stability of drinking water without disinfectant residuals in a full-scale water supply system. J Water Supply: Res and Tech. 2010 Feb;59(1):31–10.

26. Nescerecka A, Rubulis J, Vital M, Juhna T, Hammes F. Biological Instability in a Chlorinated Drinking Water Distribution Network. Balcazar JL, editor. PLoS ONE. 2014 May 5;9(5):e96354–11.

27. Prest EI, Weissbrodt DG, Hammes F, Van Loosdrecht MCM, Vrouwenvelder JS. Long-Term Bacterial Dynamics in a Full-Scale Drinking Water Distribution System. Paranhos R, editor. PLoS ONE. 2016 Oct 28;11(10):e0164445–20.

28. DeMoultrie E. Discussion about El Paso water quality goals in full-scale drinking water distribution. El Paso, TX; 2016.

29. Gomes IB, Simões M, Simões LC. An overview on the reactors to study drinking water biofilms. Water Res. Elsevier Ltd; 2014 Oct 1;62(C):63–87.

30. Wang H, Pryor MA, Edwards MA, Falkinham JO III, Pruden A. Effect of GAC pre-treatment and disinfectant on microbial community structure and opportunistic pathogen occurrence. Water Res. Elsevier Ltd; 2013 Oct 1;47(15):5760–72.

31. Revetta RP, Gomez-Alvarez V, Gerke TL, Santo Domingo JW, Ashbolt NJ. Changes in bacterial composition of biofilm in a metropolitan drinking water distribution system. J Appl Microbiol. 2016 Jun 22;121(1):294–305.

32. Gomez-Alvarez V, Schrantz KA, Pressman JG, Wahman DG. Biofilm Community Dynamics in Bench-Scale Annular Reactors Simulating Arrestment of Chloraminated Drinking Water Nitrification. Environ Sci Technol. 2014 May 2;48(10):5448–57.

33. Kantor RS, Miller SE, Kennedy LC, Nelson KL. Changes in the water microbiome through a demonstration-scale advanced treatment facility.

34. Hickel B, Sehested K. Reaction of Hydroxyl Radicals with Ammonia in Liquid Water at Elevated Temperatures. Int J Radiat Biol. 2002 Apr;39(4):355–7.

35. Bergese J. Kinetics and Benefits of Employing UV Light for the Treatment of Aqueous Ammonia in Wastewater. Gagnon G, Rand J, editors. [Halifax, Novia Scotia]; 2013.

36. Pressley TA, Bishop DF, Roan SG. Ammonia-nitrogen removal by breakpoint chlorination. Environ Sci Technol. 1972 Jul;6(7):622–8.

37. Prest EI, Hammes F, Kötzsch S, Van Loosdrecht MCM, Vrouwenvelder JS. Monitoring microbiological changes in drinking water systems using a fast and reproducible flow cytometric method. Water Res. Elsevier Ltd; 2013 Dec 1;47(19):7131–42.

38. Gatza E, Hammes F, Prest E. Assessing Water Quality with the BD Accuri™ C6 Flow Cytometer. 2013 Jan pp. 1–12.

39. Farhat N, Hammes F, Prest E, Vrouwenvelder J. A uniform bacterial growth potential assay for different water types. Water Res. Elsevier Ltd; 2018 Oct 1;142:227–35.

40. Hammes F. Assimilable Organic Carbon (AOC): Filtration Method. 2nd ed. Zurich, Switzerland; 2015. pp. 1–6.

41. Gerardi MH. Chapter 3: Bacteria. Wastewater Bacteria. John Wiley and Sons, Inc; 2006. pp. 1–267.

42. Buysschaert B, Vermijs L, Naka A, Boon N, De Gusseme B. Online flow cytometric monitoring of microbial water quality in a full-scale water treatment plant. Nat Part J Clean Water. Springer US; 2018 Aug 1;:1–7.

43. Occurrence and Fate of Ultramicrobacteria in a Full-Scale Drinking Water Treatment Plant. fmicb-09-02922tex. 2018 Dec 3;:1–14.

44. Wünsch R, Plattner J, Cayon D, Eugster F, Gebhardt J, Wülser R, Gunten von U, Wintgens T. Surface water treatment by UV/H 2O 2with subsequent soil aquifer treatment: impact on micropollutants, dissolved organic matter and biological activity. Environ Sci: Water Res Technol. Royal Society of Chemistry; 2019;5(10):1709–22.

45. Mamane H, Shemer H, Linden KG. Inactivation of E. coli, B. subtilis spores, and MS2, T4, and T7 phage using UV/H2O2 advanced oxidation. J Hazard Mater. 2007 Jul;146(3):479–86.

46. Wullings BA, Bakker G, van der Kooij D. Concentration and Diversity of Uncultured Legionella spp. in Two Unchlorinated Drinking Water Supplies with Different Concentrations of Natural Organic Matter. Appl Environ Microbiol. 2011 Jan 12;77(2):634–41.

47. Vignola M, Werner D, Wade MJ, Meynet P, Davenport RJ. Medium shapes the microbial community of water filters with implications for effluent quality. Water Res. Elsevier Ltd; 2017 Sep 22;129:499–508.

48. Le Dantec C, Duguet JP, Montiel A, Dumoutier N, Dubrou S, Vincent V. Occurrence of Mycobacteria in Water Treatment Lines and in Water Distribution Systems. Appl Environ Microbiol. 2002 Nov 1;68(11):5318–25.

49. Kotlarz NP. Factors of Full-Scale Drinking Water Treatment that Contribute to Risk of Opportunistic Infectious Disease. LiPuma JJ, Raskin LM, editors. 2017. pp. 1–158.

50. Cheswick R, Cartmell E, Lee S, Upton A, Weir P, Moore G, Nocker A, Jefferson B, Jarvis P. Comparing flow cytometry with culture-based methods for microbial monitoring and as a diagnostic tool for assessing drinking water treatment processes. Env Intern. Elsevier; 2019 Sep 1;130:104893.

51. Gillespie S, Lipphaus P, Green J, Parsons S, Weir P, Juskowiak K, Jefferson B, Jarvis P, Nocker A. Assessing microbiological water quality in drinking water distribution systems with disinfectant residual using flow cytometry. Water Res. Elsevier Ltd; 2014 Nov 15;65(C):224–34.

52. Xie X. Development of a Rapid ATP Analysis Method: Biomass Growth ATP Method for UV Disinfection Monitoring in Wastewater Treatment. Gagnon G, editor. [Halifax, Nova Scotia]; 2014. pp. 1–148.

53. Volk CJ, Lechevallier MW. Assessing biodegradable organic matter. J Am Water Works Assoc. 2000 May 1;92(5):64–76.

54. Warsinger DM, Chakraborty S, Tow EW, Plumlee MH, Bellona C, Loutatidou S, Karimi L, Mikelonis AM, Achilli A, Ghassemi A, Padhye LP, Snyder SA, Curcio S, Vecitis CD, Arafat HA, Lienhard JH V. A review of polymeric membranes and processes for potable water reuse. Prog Polym Sci. 2016 Nov 10;81:209–37.

55. Schäfer AI, Fane AG, Waite TD. Fouling effects on rejection in the membrane filtration of natural waters. Desalination. 2000 Jun;131:215–24.

56. Qu F, Wang H, He J, Fan G, Pan Z, Tian J, Rong H, Li G, Yu H. Tertiary treatment of secondary effluent using ultrafiltration for wastewater reuse: correlating membrane fouling with rejection of effluent organic matter and hydrophobic pharmaceuticals. Environ Sci: Water Res Technol. Royal Society of Chemistry; 2019;5(4):672–83.

57. Hammes F, Egli T. A flow cytometric method for AOC determination. TECHNEAU; 2007 Jul pp. 1–20. Report No.: 3.3.1.

58. Weinrich L, LeChevallier M, Haas CN. Contribution of assimilable organic carbon to biological fouling in seawater reverse osmosis membrane treatment. Water Res. Elsevier Ltd; 2016 Sep 15;101(C):203–13.

59. Park JW, Lee YJ, Meyer AS, Douterelo I, Maeng SK. Bacterial growth through microfiltration membranes and NOM characteristics in an MF-RO integrated membrane system: Lab-scale and full-scale studies. Water Res. Elsevier Ltd; 2018 Nov 1;144:36–45.

60. Bereschenko LA, Stams AJM, Euverink GJW, Van Loosdrecht MCM. Biofilm Formation on Reverse Osmosis Membranes Is Initiated and Dominated by Sphingomonas spp. Appl Environ Microbiol. 2010 Apr 2;76(8):2623–32.

61. Ihssen J. Specific growth rate and not cell density controls the general stress response in Escherichia coli. Micro. 2004 Jun 1;150(6):1637–48.

62. Kodukula PS, Prakasan TBS. Role of pH in Biological Waste Water Treatment Process. In: Bazin MJ, Prosser JI, editors. Physiological Models in Microbiology. Boca Raton; 2018. pp. 113–36.

63. Booth IR. Regulation of Cytoplasmic pH in Bacteria. Micro Reviews. 1985 Dec;49(4):359–78.

64. Sousi M, Liu G, Salinas-Rodriguez SG, Knezev A, Blankert B, Schippers JC, Gagnon G, Kennedy MD. Further developing the bacterial growth potential method for ultra-pure drinking water produced by remineralization of reverse osmosis permeate. Water Res. Elsevier Ltd; 2018 Nov 15;145:687–96.

65. Marron EL, Mitch WA, Gunten von U, Sedlak DL. A Tale of Two Treatments: The Multiple Barrier Approach to Removing Chemical Contaminants During Potable Water Reuse. Acc Chem Res. American Chemical Society; 2019 Mar 1;52(3):615–22.

66. Francisque A, Rodriguez MJ, Miranda-Moreno LF, Sadiq R, Proulx F. Modeling of heterotrophic bacteria counts in a water distribution system. WR. Elsevier Ltd; 2009 Mar 1;43(4):1075–87.

67. Lechevallier MW, Schulz W, Lee RG. Bacterial Nutrients in Drinking Water. Appl Environ Microbiol. 1991 Mar;57(3):857–62.

68. Bertelli C, Courtois S, Rosikiewicz M, Piriou P, Aeby S, Robert S, Loret J-F, Greub G. Reduced Chlorine in Drinking Water Distribution Systems Impacts Bacterial Biodiversity in Biofilms. Front Microbiol. 2018 Oct 23;9:1–11.

69. Virto R, Manas P, Alvarez I, Condon S, Raso J. Membrane Damage and Microbial Inactivation by Chlorine in the Absence and Presence of a Chlorine-Demanding Substrate. Appl Environ Microbiol. 2005 Sep 8;71(9):5022–8.

70. Liu G, Van der Mark EJ, Verberk JQJC, Van Dijk JC. Flow Cytometry Total Cell Counts: A Field Study Assessing Microbiological Water Quality and Growth in Unchlorinated Drinking Water Distribution Systems. BioMed Research International. 2013;2013(11):1–10.

71. Kerneïs A, Nakache F, Deguin A, Feinberg M. The effects of water residence time on the biological quality in a distribution network. Water Res. 1995;29(7):1719–27.

72. Dias V, Durand A-A, Constant P, Prévost M, Bédard E. Identification of Factors Affecting Bacterial Abundance and Community Structures in a Full-Scale Chlorinated Drinking Water Distribution System. Water Res. 2019 Mar;11(3):627–16.

73. Escobar IC, Randall AA. Assimilable organic carbon (AOC) and biodegradable dissolved organic carbon (BDOC). Water Res. 2001 Dec;35(18):4444–54.

74. Prest E. Biological stability in drinking water distribution systems: A novel approach for systematic microbial water quality monitoring. Vrouwenvelder JS, Van Loosdrecht MCM, editors. [Montpellier]; 2015.

75. Miettinen IT, Vartiainen T, Martikainen PJ. Phosphorus and Bacterial Growth in Drinking Water. Appl Environ Microbiol. 1997 Jul 21;63(8):3242–5.

76. Prest EI, Hammes F, van Loosdrecht MCM, Vrouwenvelder JS. Biological Stability of Drinking Water: Controlling Factors, Methods, and Challenges. Front Microbiol. 2016 Feb 1;7(41):133–24.

77. City of El Paso, El Paso Water, Chemical Analysis - City Water [Internet]. Available from: https://www.epwater.org/UserFiles/Servers/Server_6843404/File/Our%20Water/Water%20Quality/chemanalysis.pdf

78. Lechevallier MW, Cawthon CD, Lee RG. Inactivation of Biofilm Bacteria. Appl Environ Microbiol. 1988 Oct;54(10):2492–9.

1006 79. Fair GM, Morris JC, Chang SL, Weil I, Burden RP. The Behavior of Chlorine as a
1007 Water Disinfectant. J Am Water Works Assoc. 2018 Aug 31;40(10):1051–61.

1008 80. Tchobanoglous G, Olivieri A, Cotruvo J, Crook J, McDonald E, Salveson A, Trussell
1009 RS. Framework for Direct Potable Reuse. Mosher JJ, Vartanian GM, editors. 2015 p.
1010 170. Report No.: 14-20.

1011 81. Ramseier MK, Gunten von U, Freihofer P, Hammes F. Kinetics of membrane damage to
1012 high (HNA) and low (LNA) nucleic acid bacterial clusters in drinking water by ozone,
1013 chlorine, chlorine dioxide, monochloramine, ferrate(VI), and permanganate. Water Res.
1014 Elsevier Ltd; 2011 Jan 1;45(3):1490–500.

1015 82. Chan S, Pullerits K, Keucken A, Persson KM, Paul CJ, Rådström P. Bacterial release
1016 from pipe biofilm in a full-scale drinking water distribution system. npj: Biofilms
1017 Microbiomes. Springer US; 2019 Feb 16;:1–8.

1018 83. Eydal HSC, Pedersen K. Use of an ATP assay to determine viable microbial biomass in
1019 Fennoscandian Shield groundwater from depths of 3–1000 m. J Micro Methods. 2007
1020 Aug;70(2):363–73.

1021 84. Wilson CA, Stevenson H, Chrzanowski TH. The contribution of bacteria to the total
1022 adenosine triphosphate extracted from the microbiota in the water of a salt-marsh creek.
1023 J Exp Marine Bio and Ecol. 1981 Mar 16;50(2-3):183–95.

1024 85. Velten S, Hammes F, Boller M, Egli T. Rapid and direct estimation of active biomass on
1025 granular activated carbon through adenosine tri-phosphate (ATP) determination. Water
1026 Res. 2007 May;41(9):1973–83.

1027 86. Karl DM. Cellular Nucleotide Measurements and Applications in Microbial Ecology.
1028 Micro Reviews. 1980 Dec;44(4):739–96.

1029 87. Barrette WC Jr., Hannum DM, Wheeler WD, Hurst JK. General mechanism for the
1030 bacterial toxicity of hypochlorous acid: abolition of ATP production. Biochemistry.
1031 2002 May;28(23):9172–8.

1032 88. Hwang C, Ling F, Andersen GL, LeChevallier MW, Liu WT. Microbial Community
1033 Dynamics of an Urban Drinking Water Distribution System Subjected to Phases of
1034 Chloramination and Chlorination Treatments. Appl Environ Microbiol. 2012 Oct
1035 22;78(22):7856–65.

1036 89. Zamyadi A, MacLeod SL, Fan Y, McQuaid N, Dorner S, Sauvé S, Prévost M. Toxic
1037 cyanobacterial breakthrough and accumulation in a drinking water plant: A monitoring
1038 and treatment challenge. WR. Elsevier Ltd; 2012 Apr 1;46(5):1511–23.

1039 90. Chrysovergi A. Ammonium Removal by Reverse Osmosis Membranes. Gagnon G,
1040 editor. [Delft, Netherlands]; 2016. pp. 1–161.

91. Tchobanoglous G. Integrated wastewater management: The future of water reuse in large metropolitan areas. Integr Environ Assess Manag. 2018 Dec 27;15(1):160–3.

92. Bernados B. Reverse Osmosis for Direct Potable Reuse in California. J Am Water Works Assoc. 2018 Jan;110(1):28–36.

93. Olivieri A, Crook J, Anderson M, Bull R, Drewes J, Haas CN, Jakubowski W, McCarty PL, Nelson KL, Rose JB, Sedlak DL, Wade T. Evaluation of the Feasibility of Developing Uniform Water Recycling Criteria for Direct Potable Reuse. 2016 Aug pp. 1–420.

94. Fujioka T, Hoang AT, Aizawa H, Ashiba H, Fujimaki M, Leddy M. Real-Time Online Monitoring for Assessing Removal of Bacteria by Reverse Osmosis. Environ Sci Technol Lett. American Chemical Society; 2018 Apr 26;5(6):389–93.

95. Besmer MD, Weissbrodt DG, Kratochvil BE, Sigrist JA, Weyland MS, Hammes F. The feasibility of automated online flow cytometry for in-situ monitoring of microbial dynamics in aquatic ecosystems. Front Microbiol. 2014 Jun 2;5(265):1–12.

96. Besmer MD, Epting J, Page RM, Sigrist JA, Huggenberger P, Hammes F. Online flow cytometry reveals microbial dynamics influenced by concurrent natural and operational events in groundwater used for drinking water treatment. Sci Rep. Nature Publishing Group; 2016 Nov 24;6:38462:1–10.

97. Chuang Y-H, Chen S, Chinn CJ, Mitch WA. Comparing the UV/Monochloramine and UV/Free Chlorine Advanced Oxidation Processes (AOPs) to the UV/Hydrogen Peroxide AOP Under Scenarios Relevant to Potable Reuse. Environ Sci Technol. 2017 Nov 21;51(23):13859–68.

98. Zhang Z, Chuang Y-H, Szczuka A, Ishida KP, Roback S, Plumlee MH, Mitch WA. Pilot-scale evaluation of oxidant speciation, 1,4-dioxane degradation and disinfection byproduct formation during UV/hydrogen peroxide, UV/free chlorine and UV/chloramines advanced oxidation process treatment for potable reuse. Water Res. 2019 Nov;164:114939–51.

99. Zeng T, Plewa MJ, Mitch WA. N-Nitrosamines and halogenated disinfection byproducts in U.S. Full Advanced Treatment trains for potable reuse. Water Res. Elsevier Ltd; 2016 Sep 15;101(C):176–86.

100. Tchobanoglous G, Leverenz H. Comprehensive Source Control for Potable Reuse. Front Environ Sci. 2019 Jun 20;7:782–12.

101. Gerrity D, Owens-Bennett E, Venezia T, Stanford BD, Plumlee MH, Debroux J, Trussell RS. Applicability of Ozone and Biological Activated Carbon for Potable Reuse. Ozone: Science & Engineering. 2014 Apr 14;36(2):123–37.

102. Liu C, Olivares CI, Pinto AJ, Lauderdale CV, Brown J, Selbes M, Karanfil T. The control of disinfection byproducts and their precursors in biologically active filtration processes. WR. Elsevier Ltd; 2017 Nov 1;124:630–53.

103. Lehman CL, Tilman D. Biodiversity, Stability, and Productivity in Competitive Communities. The American Naturalist. 2000 Nov;156(5):534–52.

104. Briones A, Raskin L. Diversity and dynamics of microbial communities in engineered environments and their implications for process stability. Current Opinion in Biotechnology. 2003 Jun;14(3):270–6.

Wastewater Treatment

Advanced Treatment

Distribution System

How many cells? How viable are they?
How much potential for growth?